Article

Conventional and Advanced Exergoeconomic Analysis of a Compound Ejector-Heat Pump for Simultaneous Cooling and Heating

Ali Khalid Shaker Al-Sayyab [1,2,*], **Joaquín Navarro-Esbrí** [1,*], **Victor Manuel Soto-Francés** [3,*] **and Adrián Mota-Babiloni** [1,*]

[1] ISTENER Research Group, Department of Mechanical Engineering and Construction, Universitat Jaume I, Campus de Riu Sec s/n, 12071 Castelló de la Plana, Spain

[2] Thermal Mechanical Engineering, Basra Engineering Technical College (BETC), Southern Technical University, 61004 Basra, Iraq

[3] Departamento de Termodinámica Aplicada, Universitat Politècnica de València, Camino de Vera s/n, 46022 Valencia, Spain

[*] Correspondence: ali.alsayyab@stu.edu.iq (A.K.S.A.-S.); navarroj@uji.es (J.N.-E.); vsoto@ter.upv.es (V.M.S.-F.); mota@uji.es (A.M.-B.)

Abstract: This work focused on a compound PV/T waste heat driven ejector-heat pump system for simultaneous data centre cooling and waste heat recovery for district heating. The system uses PV/T waste heat as the generator's heat source, acting with the vapour generated in an evaporative condenser as the ejector drive force. Conventional and advanced exergy and advanced exergoeconomic analyses are used to determine the cause and avoidable degree of the components' exergy destruction rate and cost rates. Regarding the conventional exergy analysis for the whole system, the compressor represents the largest exergy destruction source of 26%. On the other hand, the generator shows the lowest sources (2%). The advanced exergy analysis indicates that 59.4% of the whole system thermodynamical inefficiencies can be avoided by further design optimisation. The compressor has the highest contribution to the destruction in the avoidable exergy destruction rate (21%), followed by the ejector (18%) and condenser (8%). Moreover, the advanced exergoeconomic results prove that 51% of the system costs are unavoidable. In system components cost comparison, the highest cost comes from the condenser, 30%. In the same context, the ejector has the lowest exergoeconomic factor, and it should be getting more attention to reduce the irreversibility by design improving. On the contrary, the evaporator has the highest exergoeconomic factor (94%).

Keywords: advanced exergy; exergoeconomic; compound ejector-vapour compression; data centre cooling; district heating; photovoltaic thermal (PV/T)

1. Introduction

By 2050, the European Union's target is to become climate neutral by increasing renewable energy dependence and improving energy efficiency by recovering waste heat [1,2]. Information and communications technology (ICT) represents an emerging sector because its energy consumption value is 2.5% of European Union electricity consumption [3].

The Internet of Things (IoT) provides various services to its users, such as data management, storage, and usage. However, IoT often requires data centres, increasing power demand between 15% and 20% [4]. Reducing energy consumption and costs in a data centre is a challenging issue because the performance and lifetime of electronic components are susceptible to indoor conditions. The data centre cooling system represents 40% of the total consumption [5].

Conventional heat pumps are considered a flexible option in data centres because they can regulate the cooling capacity according to the load demand. Furthermore, they can be combined with other promising green technologies.

Subsequent research and developments have resulted in the development of heat pumps that efficiently use existing resources. One of these advancements is that they can produce heating and cooling simultaneously [6], saving electricity compared to traditional heat pumps [7]. Another benefit is they can run connected to photovoltaic-thermal (PV/T) panels (so-called solar assisted heat pumps), so the consumption power is reduced because they operate at higher evaporating temperatures. Meanwhile, the generated electric power is used to operate the heat pump compressor [8]. Recently, heat pumps have been combined to waste heat-driven ejectors, presenting a system performance enhancement [9].

Usually, the exergy analysis is combined with energy modelling and simulation techniques. It allows identifying the sources of thermodynamics' irreversibility in heat pumps for optimising performance. Fu et al. [10] presented an energy and exergy assessment of a solar-assisted R-134a heat pump system operated in three modes: heat-pipe, air-source heat pumps and solar-assisted, presenting the latter with the highest average daily exergy efficiencies, around 7.6%. Zhang et al. [11] concluded that a 735 W R-134a PV/T-loop heat-pipe heat pump presents a 15% exergy efficiency with a 5.5 COP. Xu et al. [12] obtained an R-152a modified system that presents an energy-saving with higher exergy performance than a conventional ejection-compression refrigeration cycle. Chen et al. [13] showed that the ejector represents the highest source of irreversibility for different ejector cooling system arrangements, followed by the generator and evaporator.

Components of complex systems are affected reciprocally. Therefore, none of the conventional exergy analyses can accurately estimate the sources of irreversibility or evaluate the performance enhancement potential. Meanwhile, knowledge of system components' interactions helps prevent misguiding in energy enhancement strategies [14]. A powerful technique named 'advanced exergy analysis' [15] gives further understanding in evaluating the magnitudes and sources of exergy destruction with the consequent exergy analysis accuracy improvement. In the advanced exergy method, the endogenous/exogenous exergy destruction indicates the capability of determining the irreversibility due to system component interactions. On the other hand, the unavoidable/avoidable exergy destruction can evaluate the irreversibility to be reduced by design modifications and optimisation. This separation makes exergy contribute to the understanding and manipulation for thermal system improvement [16].

Recently, researchers have started to apply advanced exergy methods to thermal systems, including heat pumps with different purposes. Morosuk et al. [17] concluded that R-125, R-134a, R-22, R717, R-500, and R-407C have a comparable ratio of advanced exergy destruction splitting in a simple vapour compression cycle, and the highest exergy destruction occurs in the condenser, followed by the compressor. Meanwhile, the evaporator and the expansion valve have the highest avoidable and unavoidable endogenous exergy destruction ratio, respectively. Erbay et al. [18] presented an advanced exergy analysis for a ground-source heat pump for drying processes. The internal operating conditions have inefficiencies on all components, except for the condenser and evaporator.

Other studies adopted the advanced exergy evaluation for ejector cooling systems and compound ejector heat pump system. Chen et al. [19] indicated that 50% of total exergy destruction arises from the ejector, while the generator causes 25%. Zhao et al. [20] studied parallel and series compressor–ejector arrangements showing that the highest avoidable endogenous exergy destruction ratio is reported to both compressor and ejector. Gullo [21] applied advanced exergy analysis to transcritical R744 supermarket refrigeration systems with three arrangements: parallel compression, parallel compression with two-phase ejectors-overfed evaporators, and without two-phase ejectors. The ejector arrangement shows a total irreversibilities reduction of 9.3% and 13.5% avoidable destruction.

A new method involving advanced exergy analysis with economic restrictions (exergoeconomic analysis) has recently been adopted to optimise system performance with an

accuracy not possible by conventional approaches [14]. Sing h et al. [16] observed that both expansion device and evaporator need optimisation for solar-assisted and conventional heat pumps for drying purposes. Ambriz-Díaz et al. [22] considered a polygeneration plant operated by a geothermal cascade arrangement. The results indicate that the exergy destruction in the heat exchanger and in the ORC can be avoided by improving these design variables. Hepbasli et al. [23] studied a pilot-scale air-source heat pump for food drying. They concluded that the advanced exergoeconomic analysis gives a more sensitive evaluation of inefficient components to system modification and efficiency improvement. On the other hand, cost-reducing for both heat recovery and condenser units should be improved.

According to the state-of-art revision, none of the previous studies focused on the advanced exergy and exergoeconomic analyses for advanced heat pumps, neither for these systems combined with other technologies. This work presents an advanced exergoeconomic evaluation for a new arrangement of combined ejector-solar assisted heat pump system to give a complete overview of the system's potential. The new system arrangement is applied to data centre cooling and district heating simultaneously. It combines four promising technologies: a heat pump, ejector, PV/T panels, and waste heat recovery. The proposed system presents the novelty of employing PV/T waste heat with the evaporative condenser as a full ejector driving force, avoiding a pump's need. The surplus PV/T generated electricity can be used to operate the heat pump, which is cooling a data centre and injecting heat in a district heating network at the same time.

The current study's objective is to perform conventional and advanced exergoeconomic analyses for the investigated combined ejector-solar assisted heat pump system. The exergetic destruction values and unitary exergoeconomic costs for each component were determined and discussed. This will allow us to identify the magnitude and location of the most relevant thermodynamic cost losses and provide critical insights to improve the inefficient components to be more effective and reliable.

2. System Description

The system components layouts and pressure-enthalpy diagrams of the compound PV/T waste heat-driven ejector-heat pump system are shown in Figure 1a,b, respectively. The compound PV/T waste heat-driven ejector-heat pump system comprises a compressor, condenser, flash tank, high-pressure expansion valves, evaporative-condenser, PV/T waste heat exchanger-generator, ejector, low-pressure expansion valve, evaporator, as well as three brine side fluid paths for PV/T-generator, evaporator, and condenser. The refrigerant has the transformations as exposed in the following paragraphs.

Superheated refrigerant enters the compressor at the intermediate pressure (State 1), and is compressed and delivered at condenser pressure. The high-pressure superheated refrigerant enters the condenser. The condensation process occurs by rejecting heat to the district heating system's heat sink (State 3); in the next stage, the cold liquid–gas mixture goes through the flash tank to undergo an adiabatic phase separation at the condenser pressure. The refrigerant leaves the flash tank from the bottom as saturated liquid (State 5) (primary flow) and from the upper side as saturated vapour (State 4) (secondary flow). Then, the high-pressure liquid refrigerant expands through the high-pressure expansion valve in the next stage, resulting in a mixture of liquid and gas at lower pressure and lower temperatures (State 5').

After that, the two streams of refrigerant pass through an evaporative-condenser, which is used to condense the vapour stream from the flash tank separator (secondary flow), exchanging heat with a low-temperature stream (primary flow) after the first throttling process (Expansion Valve I). The primary stream leaves the evaporative condenser in a mixture state at generator pressure (State 6). It then enters the generator, where it is evaporated by exchanging heat from the cooling water of the PV/T waste heat recovery coil. Furthermore, the bypass vapour stream's cooling effect could be utilised at the evaporative condenser and delivered as a liquid refrigerant to the second expansion valve (the

secondary flow), expanding through the low-pressure expansion valve. From this, a mixture exits at evaporator pressure (State 8'). It removes heat load from the data centre using the evaporator cooling water. It is wholly evaporated in the final stage before returning to the ejector suction nozzle (State 9) and exits superheated.

On the other hand, the refrigerant leaves the generator. After being superheated (State 7) it is shunted to the ejector's primary nozzle, representing the most considerable refrigerant mass flow rate of the motive flow entering the nozzle and enhancing the pressure lift effect. The primary stream expands through the nozzle and exits at low pressure. It creates an evacuation force for the low-pressure vapour (secondary flow). The two streams undergo a constant pressure mixing process (State M) and introduce normal shock trains in the mixing section. Meanwhile, the pressure recovery process takes place in the diffuser section of the ejector. The mixed stream enters the compressor (State 1), where the cycle starts again.

The system is designed to cover three functions. First, the PV/T operating temperature is decreased, and the generated electric power is maximised. This waste heat is used as the generator's heat source, acting with the vapour generated in an evaporative condenser as the ejector drive force. The second function is to absorb the data centre's waste heat generated and maintain the indoor air conditions in the ASHRAE comfort zone. Finally, this heat is upgraded to the compressor's functional temperature levels, specifically for district heating.

The arrangement yields high system performance due to overall exergy destruction optimisation by the ejector's arrangement, allowing electricity saving by reducing the compressor's pressure ratio and its irreversibility. Combining an evaporative-condenser leads to improving the system overall exergy destruction by removing the ejector's pump (absence of pump exergy destruction). Moreover, the condenser waste heat is used in the auxiliary heat exchanger to compensate for the absence of solar intensity (overcast day conditions).
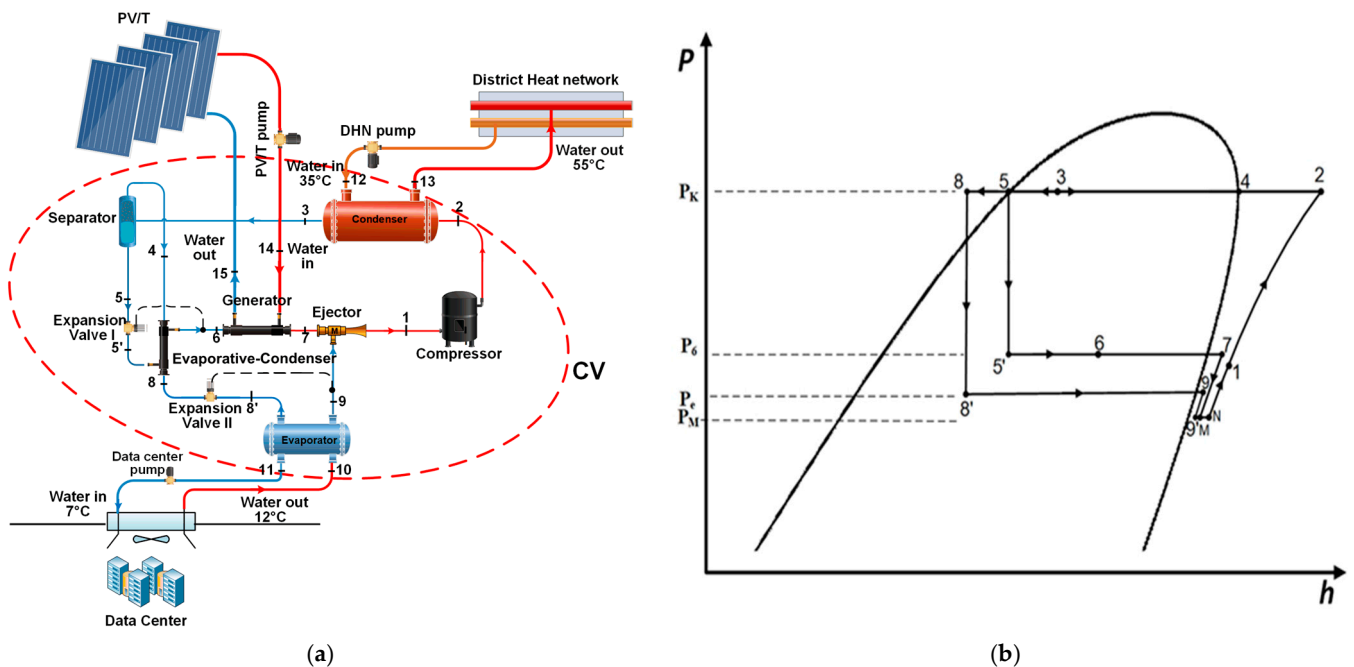

Figure 1. Proposed solar-driven ejector-compression system: (**a**) schematic, and (**b**) P-h diagram.

3. Methodology

3.1. System Modelling

The flow chart indicating the methodology employed for calculating energetic performances, conventional exergy, and advanced exergoeconomic analysis for the compound ejector heat pump is shown in Figure 2. The real, ideal, and unavoidable cycles conditions are established by selecting the parameters listed in Table 1. Then, the thermodynamic system parameters are obtained using the energetic system model.

The energetic system model includes all the energy, exergy, economical, and advanced exergy and exergoeconomic equations required. Moreover, four sub-models are employed, so the ejector, evaporative-condenser, PV/T, and heat exchangers area model are connected to the primary model to complete the entire system evaluation. An iteration loop's ejector outlet's pressure is evaluated with a relative convergence tolerance of 0.1% in the ejector model. Moreover, in the evaporative-condenser heat exchange model, an iteration loop is adopted with a relative convergence tolerance of 0.1%, while for the PV/T, the relative convergence tolerance is 0.5%.

The system performance parameters for real, ideal, and unavoidable conditions could be obtained to perform the advanced energy–exergy cycle performance evaluation by knowing the system energy parameters like mass flow rate and the specific enthalpy, specific entropy, and exergy destruction. What is more, endogenous/exogenous and avoidable/unavoidable exergy destruction can be gained by further calculation.

Finally, by evaluating the components' sizing in real and unavoidable conditions, advanced exergoeconomic evaluations are adopted for all system components. The exergoeconomic analysis requires several thermodynamic and transport properties, which still have not been included for recently commercialised refrigerants (such as R1234ze (E)) in the most used software (EES [24] and REFPROP [25]). However, these properties are available for R134a, which is the most representative refrigerant for chillers. Therefore, R-134a is selected as the heat pump working fluid. The Engineering Equation Solver (EES) software [24] is used to model the proposed system and introduce all assumptions, boundary conditions, and inputs.
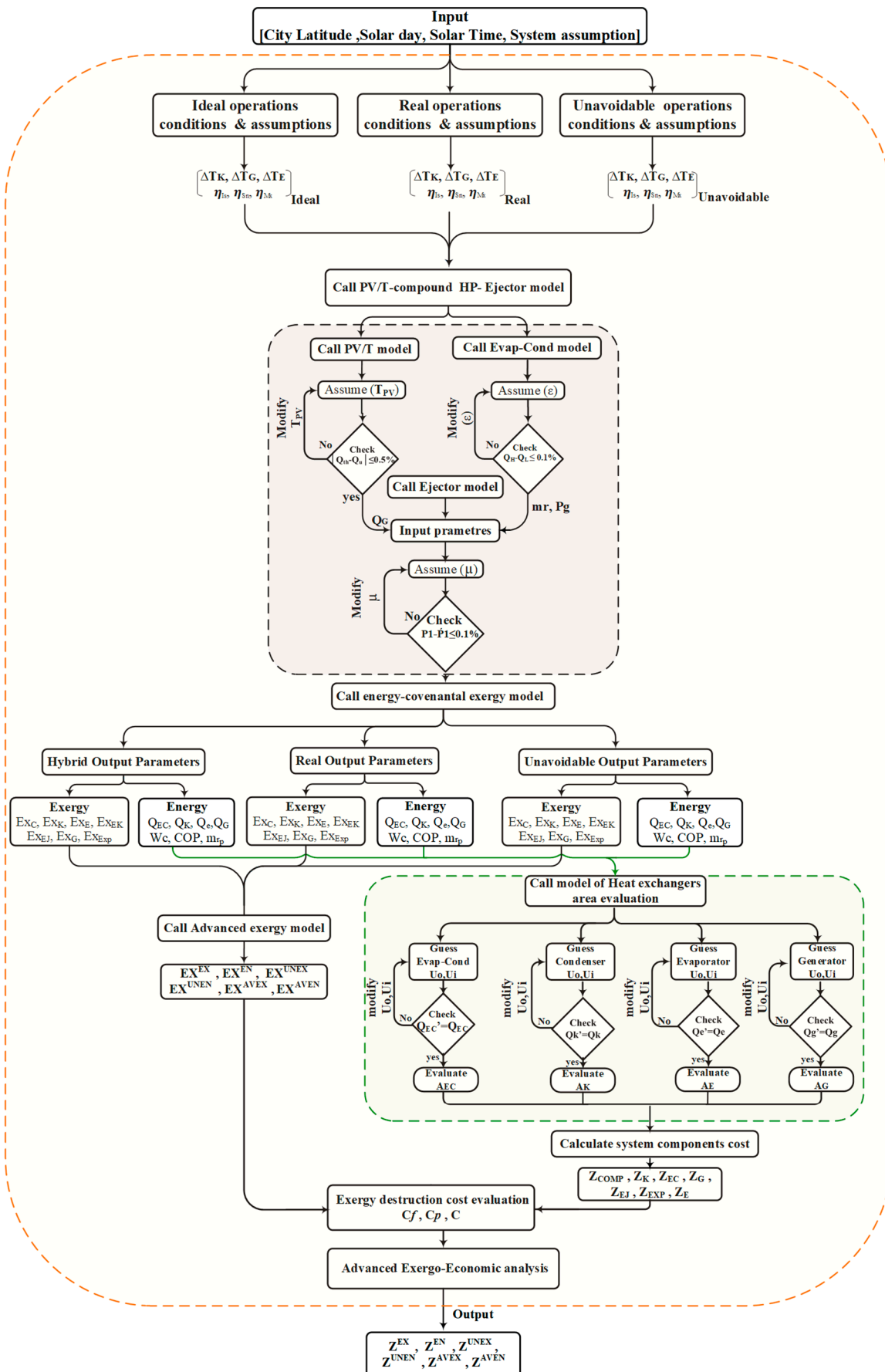
Figure 2. Flow diagram for the system methodology.

3.2. Boundary Conditions and Assumptions

The ambient air temperatures and hourly solar intensity are based on Valencia (Spain) actual data [26] and considered input parameters. The evaporator's temperature difference and cooling load for the data centre cooling system are 5 °C and 90 kW, respectively. The refrigerant quality at the condenser outlet (x_3) is fixed at 0.3 to achieve relatively high system performance and avoid the two-phase flow at the compressor inlet at very low solar intensity. The refrigerant state leaving the flash tank is a saturated vapour and liquid from the upper and bottom parts, respectively. Besides that, the saturated liquid is delivered to the first and second expansion valve. Pressure drops and heat transfer to the surrounding through the connection pipes and compressor are neglected. In the advanced exergy analysis, hypered condition requires a match in cooling and heating capacity. Therefore, the water's inlet and outlet temperatures at the evaporator and condenser are kept at 12 °C–7 °C ($\Delta T_{Ew} = 5$ °C) and 35 °C–55 °C ($\Delta T_{Kw} = 20$ °C), respectively.

The quantitative sensitivity study varies one parameter while keeping constant the remaining. Therefore, the condensing and evaporator glide is varied from 4.5 to 9 °C and 3 to 7.5 °C, respectively. On the other hand, the compressor mechanical efficiency is varied from 0.7 to 0.88 and finally, the ejector efficiencies (η_D, η_{pn}, η_{MX}, η_{sn}) go from 0.78 to 0.85. Table 1 summarises parameters for real, ideal, and unavoidable cycle conditions. Table 2 summarises the main assumptions and boundary condition.

Table 1. Parameters for real, ideal, and unavoidable cycle conditions [9,20].

Components	Parameters	Real	Ideal	Unavoidable
Compressor	η_M	78%	100%	95%
Condenser	ΔT_K	5 °C	0 °C	0.5 °C
	ΔT_{Kw}	20 °C	20 °C	20 °C
Generator	ΔT_G	5 °C	0 °C	0.5 °C
Evaporative-Condenser	ΔT_{EC}	3 °C	0 °C	0.3 °C
Evaporator	ΔT_E	5 °C	0 °C	0.5 °C
	ΔT_{Ew}	5 °C	5 °C	5 °C
Expansion Valve		Isenthalpic	Isentropic	Isenthalpic
Ejector	η_{pn}	85%	100%	94%
	η_{sn}	84%	100%	92%
	η_D	87%	100%	95%
	η_{MX}	79%	100%	86%

Table 2. Assumptions and boundary conditions.

Parameters	Assumed Value
Condensing temperature	60 °C
Evaporating temperature	2 °C
D_{ok}	28 mm
D_{ik}	26.35 mm
D_{oe}	20 mm
D_{ie}	18.35 mm
PV/T area	1.65 X1.3 X 350 m^2
Data centre cooling load	90 kW
Compressor rotational speed	2900 rpm
V_{DS}	0.001936 m^3
n	15 years
α	5040 h (Valencia, Spain)

3.3. Model Equations

The advanced exergy analysis provides additional helpful information that cannot be obtained through conventional energy–exergy analysis and economic analysis [27]. The source of thermodynamic inefficiencies, irreversibility of the components, system cost, and exergoeconomic analysis are calculated. It identifies the most present cost-effective ways to improve the system performance.

3.3.1. Energetic Model

The compressor power consumption can be obtained using Equation (1).

$$\dot{W}_c = \frac{\eta_{em}}{\eta_{is}}\,\dot{m}_r\big(\bar{h}_{c,out} - h_{c,in}\big) \tag{1}$$

The delivered refrigerant's mass flow rate is evaluated by Equation (2).

$$\dot{m}_r = \frac{\eta_v V_{DS} rpm}{v} \tag{2}$$

The compressor volumetric efficiency and isentropic efficiency are calculated as follows [28,29], Equations (3) and (4).

$$\eta_v = 0.9 - 0.035\frac{p_d}{p_s} \tag{3}$$

$$\eta_{is} = 0.976695 - 0.0366432\frac{p_d}{p_s} + 0.0013378\left(\frac{p_d}{p_s}\right)^2 \tag{4}$$

From multiplying the refrigerant specific enthalpy difference across the condenser by the refrigerant mass flow rate, the condenser heating capacity can be calculated, Equation (5).

$$\dot{Q}_k = \dot{m}_r\big(h_{k,out} - h_{k,in}\big) \tag{5}$$

The evaporative-condenser effectiveness can be obtained as indicated in Equation (6).

$$\varepsilon_{ek} = \frac{h_{in,h} - h_{out,h}}{h_{in,h} - h_{in,l}} \tag{6}$$

The ejector is a crucial component in the compound ejector compression cycle; hence, the ejector performance prediction model's accuracy severely affects the overall system performance. Up to this day, the constant pressure model was widely accepted [29–31]. Therefore, this model is adopted in thermodynamic performance evaluation.

In the ejector analysis, the most critical factor is the entrainment ratio, which can be calculated employing Equation (7).

$$\mu = \frac{\dot{m}_s}{\dot{m}_p} \tag{7}$$

The primary nozzle refrigerant exit velocity can be obtained using Equation (8) based on the energy conservation law.

$$\omega_{pn} = \sqrt{2(h_{(pn)i} - h_{(pn)ea})} \tag{8}$$

Similarly, the secondary nozzle refrigerant exit velocity can be obtained following Equation (9).

$$\omega_{sn} = \sqrt{2(h_{(sn)i} - h_{(sn)ea})} \tag{9}$$

By applying momentum and energy conservation equations on the mixing section, refrigerant conditions at the nozzle mixing section can be obtained by Equation (10) and Equation (11), respectively.

$$\omega_m = \sqrt{\eta_m}\left(\omega_{sn}\left(\frac{\mu}{1+\mu}\right) + \omega_{pn}\left(\frac{1}{1+\mu}\right)\right) \tag{10}$$

$$h_m = \frac{1}{1+\mu}\left(h_{(pn)ea} + \frac{\omega_{pn}^2}{2}\right) + \frac{\mu}{1+\mu}\left(h_{(sn)ea} + \frac{\omega_{sn}^2}{2}\right) - \frac{\omega_m^2}{2} \tag{11}$$

The ejector outlet enthalpy can be obtained from Equation (12).

$$h_{d,ea} = h_m + \frac{\omega_m^2}{2} \tag{12}$$

Finally, the nozzle and diffuser efficiency can be calculated through Equation (13) and Equation (14), respectively.

$$\eta_{ns} = \frac{h_i - h_{ea}}{h_i - h_{es}} \tag{13}$$

$$\eta_d = \frac{h_{d,es} - h_m}{h_{d,ea} - h_m} \tag{14}$$

The system energy efficiency ratio (EER) and coefficient of performance (COP) results from Equation (15) and Equation (16), respectively.

$$EER = \frac{\dot{Q}_e}{\dot{W}_c} \tag{15}$$

$$COP = \frac{\dot{Q}_k}{\dot{W}_c} \tag{16}$$

3.3.2. Conventional Exergy Model

In the conventional exergy analysis, the concept of "fuel exergy-product exergy" is used. It is noted that the fuel exergy is the exergy expended on a component (such as compressor work exergy in heat pump compressor). Besides that, the product exergy indicates the system's required exergy (such as heat supply exergy by the condenser in the heat pump). A control volume is adopted without accounting for the PV/T panels and data centre room. Ambient temperature and pressure are taken as dead state conditions. The general exergy balance equation applied to the term "fuel exergy-product exergy and exergy destruction" can be expressed as indicated in Equations (17) and (18) [32].

$$\dot{EX}_D = \dot{EX}_f - \dot{EX}_p \tag{17}$$

$$\dot{EX} = \dot{m}(h - h_0 - T_0(s - s_0)) \tag{18}$$

The detailed definition equations of the fuel exergy, product exergy, and the exergy destruction rate for each component are listed in Table 3. The system's total exergy destruction is the summation of all components, Equation (19).

$$\dot{EX}_{D,t} = \dot{EX}_{D,c} + \dot{EX}_{D,k} + \dot{EX}_{D,ek} + \dot{EX}_{D,g} + \dot{EX}_{D,ej} + \dot{EX}_{D,ex} + \dot{EX}_{D,e} \tag{19}$$

The exergy efficiency is presented in Equation (20).

$$\eta_{II} = 1 - \frac{\dot{EX}_{D,t}}{\dot{EX}_f} \tag{20}$$

Table 3. Definition of fuel, production, and exergy destruction rates of the system components [32].

Component	Exergy of Fuel	Exergy of Product	Exergy Destruction
Compressor	$\dot{EX}_{F,C} = \dot{w}_c$	$\dot{EX}_{P,C} = \dot{EX}_2 - \dot{EX}_1$	$\dot{EX}_{D,C} = \dot{EX}_{F,C} - \dot{EX}_{P,C}$
Condenser	$\dot{EX}_{F,K} = \dot{EX}_2 - \dot{EX}_3$	$\dot{EX}_{P,K} = \dot{EX}_{12} - \dot{EX}_{13}$	$\dot{EX}_{D,K} = \dot{EX}_{F,K} - \dot{EX}_{P,K}$
Expansion valve I	$\dot{EX}_{F,ex1} = \dot{EX}_5$	$\dot{EX}_{P,ex1} = \dot{EX}_{5'}$	$\dot{EX}_{D,ex1} = \dot{EX}_{F,ex1} - \dot{EX}_{P,ex1}$
Evaporative-Condenser	$\dot{EX}_{F,ec} = \dot{EX}_4 - \dot{EX}_8$	$\dot{EX}_{P,ec} = \dot{EX}_{5'} - \dot{EX}_6$	$\dot{EX}_{D,ec} = \dot{EX}_{F,ec} - \dot{EX}_{P,ec}$
Generator	$\dot{EX}_{F,G} = \dot{EX}_{14} - \dot{EX}_{15}$	$\dot{EX}_{P,G} = \dot{EX}_6 - \dot{EX}_7$	$\dot{EX}_{D,G} = \dot{EX}_{F,G} - \dot{EX}_{P,G}$
Ejector	$\dot{EX}_{F,ej} = \dot{EX}_9 - \dot{EX}_1$	$\dot{EX}_{P,ej} = \dot{EX}_1 - \dot{EX}_7$	$\dot{EX}_{D,C} = \dot{EX}_{F,ej} - \dot{EX}_{P,ej}$
Expansion valve II	$\dot{EX}_{F,ex2} = \dot{EX}_8$	$\dot{EX}_{P,ex2} = \dot{EX}_{8'}$	$\dot{EX}_{D,ex2} = \dot{EX}_{F,ex2} - \dot{EX}_{P,ex2}$

3.3.3. Economic Model

A detailed economic analysis based on the construction-maintenance cost and annual operating cost is adopted in this section. The levelisation cost method is utilised to convert the annual variable costs to equivalent constant expenses. The plant cost rate ($\dot{Z}_{CR}$) parameter can be evaluated using Equation (21) [33,34].

$$\dot{Z}_{CR} = \sum_k (\dot{Z}_{CM} + \dot{Z}_{OP}) \tag{21}$$

The construction and maintenance cost rate ($\dot{Z}_{CM}$) is calculated as shown in Equation (22).

$$\dot{Z}_{CM} = \left(\frac{IR(1+IR)^n}{(1+IR)-1}\right)\frac{Z_K}{\alpha} \tag{22}$$

Moreover, the capital construction cost functions of each component (Z) are listed in Table 4.

The equation for the operational cost rate is provided in Equation (23).

$$\dot{Z}_{OP} = \dot{Z}_{CM} \, \varphi \tag{23}$$

Table 4. Cost functions of various equipment [35,36].

System Component	Capital Cost Function
Compressor	$Z_c = 9624.2 \, \dot{W}_c^{0.46}$
Heat Exchanger	$Z_{HX} = 1397 A^{0.89}$
Expansion valve	$Z_{exp} = 114.5 \, \dot{m}_r$
Ejector	$Z_{ej} = 750 \, \dot{m}_p \, p_{de}^{-0.75} \left(\frac{T_g}{P_g}\right)^{0.05}$

The models mentioned in Duffie et al. [37], Al-Sayyab et al. [38], Bahaidarah et al. [39], and Tiwari et al. [40] are used to evaluate the effect of hourly variations of solar intensity and ambient temperatures on PV/T performance. Besides, the models mentioned in Lee [41], Thulukkanam [42], and Khosravi et al. [43] are used to predict the heat transfer coefficient's overall heat exchangers area's evaluation.

3.3.4. Conventional Exergoeconomic Model

The exergoeconomic analysis is a combination of exergy principles with economic concepts. Exergoeconomic analysis represents a powerful tool capable of estimating each

exergy stream's cost in each component by considering both capital investment costs and operation-maintenance costs [44].

By the exergoeconomic aspects, the cost balance equation is written as Equation (24) indicates [44].

$$\dot{C}_f + \dot{Z}_{CR} = \dot{C}_p \tag{24}$$

The equation of cost rate balance for each system component is listed in Table 5.

The cost rate of exergy destruction can be expressed by following Equation (25).

$$\dot{C}_D = c_f \dot{EX}_D \tag{25}$$

Finally, the total cost is calculated through Equation (26).

$$\dot{Z}_T = \dot{C}_D + \dot{Z}_{CR} \tag{26}$$

The exergoeconomic factor is the ratio of the component to total component cost, taking into account the exergy destruction cost [43], Equation (27).

$$f = \frac{\dot{Z}_{CR}}{\dot{Z}_T} \tag{27}$$

Table 5. Exergy cost equations for different components.

System Component	Equation of Cost	Auxiliary Equation
Compressor	$\dot{Z}_c + \dot{C}_1 + \dot{C}_w = \dot{C}_2$	–
Condenser	$\dot{Z}_k + \dot{C}_{12} + \dot{C}_2 = \dot{C}_{13} + \dot{C}_3$	$c_3 = c_2, c_{13} = c_{14}$
Expansion valve I	$\dot{Z}_{expI} + \dot{C}_5 = \dot{C}_{5\prime}$	–
Evaporative -Condenser	$\dot{Z}_{EC} + \dot{C}_4 + \dot{C}_{5\prime} = \dot{C}_6 + \dot{C}_8$	$c_{5\prime} = c_6$
Generator	$\dot{Z}_G + \dot{C}_6 + \dot{C}_{14} = \dot{C}_7 + \dot{C}_{15}$	$c_6 = c_7, c_{14} = c_{15}$
Ejector	$\dot{Z}_{ej} + \dot{C}_7 + \dot{C}_9 = \dot{C}_1$	–
Expansion valve II	$\dot{Z}_{expII} + \dot{C}_8 = \dot{C}_{8\prime}$	–
Evaporator	$\dot{Z}_e + \dot{C}_{11} + \dot{C}_{8\prime} = \dot{C}_9 + \dot{C}_{10}$	$c_{8\prime} = c_9, c_{11} = c_{10}$

3.3.5. Advanced Exergy Analysis

The conventional exergetic analysis does not indicate the reasons that caused exergy destruction. A recently developed technique, 'advanced exergetic analysis', can evaluate the system components' mutual interdependencies, providing helpful information for improving the system components [14].

The exergy destruction in the system components splits into two approaches, endogenous/exogenous or unavoidable/avoidable parts.

The exogenous/endogenous exergy splitting can be adopted by using the hypered cycle to the kth component. The specific component undergoes the consideration functions with its actual conditions; meanwhile, the rest of the components work in ideal conditions [19], Figure 3 shows the adopted system under the three operating conditions (Ideal, Real, and unavoidable). It allows evaluating the influence of the rest components on the exergy destruction of a specific component. The component exergy destruction depends not only on the irreversibility of a specific component, but also on the interconnections among the rest of the components [45]. The exogenous/endogenous exergy splitting can be written as shown in Equation (28).

$$\dot{E}x_{D,k} = \dot{E}x_{D,k}^{EX} + \dot{E}x_{D,k}^{EN} \tag{28}$$

$\dot{E}x_{D,k}^{EN}$ represents the internal thermal inefficiencies that can be diminished through optimisation of the performance of the specific component, while $\dot{E}x_{D,k}^{EX}$ indicates that for the other components.

Unavoidable exergy evaluation can be adopted using an unavoidable cycle that operates under best-operating conditions with zero irreversibility or minimum exergy destruction as possible (unavoidable conditions), as shown in Figure 3c, which can be expressed as indicated in Equation (29).

$$\dot{E}x_{D,k} = \dot{E}x_{D,k}^{UN} + \dot{E}x_{D,k}^{AV} \tag{29}$$

The value of the unavoidable exergy destruction with the kth component follows Equation (30).

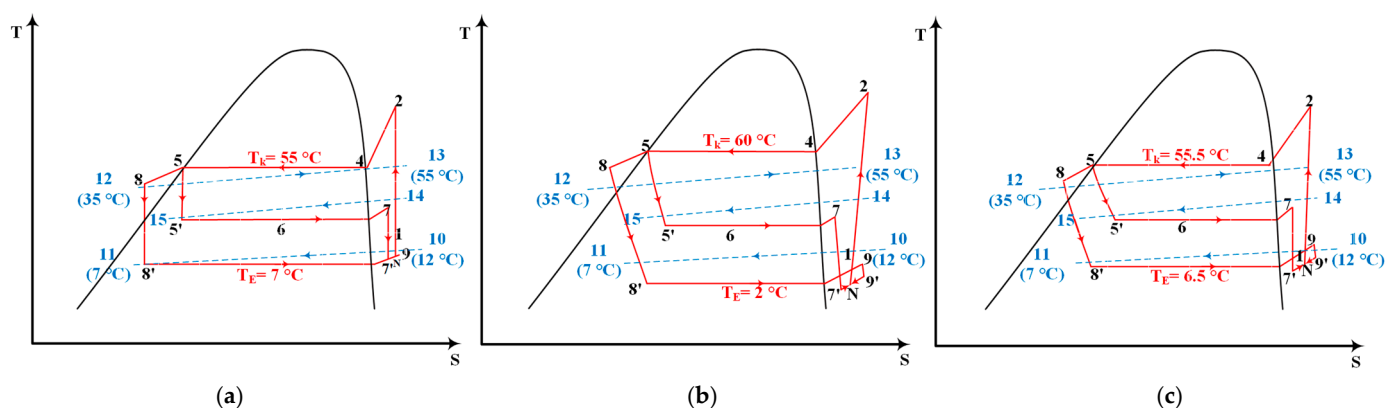$$\dot{E}x_{D,k}^{UN} = \left(\frac{\dot{E}x_{D,k}}{\dot{E}x_{P,k}}\right)^{UN} \dot{E}x_{P,k} \tag{30}$$

Figure 3. T-s diagram of the investigated system under different conditions: (**a**) ideal, (**b**) real, and (**c**) unavoidable.

The unavoidable exergy destruction ($\dot{E}x_{D,k}^{UN}$) represents the part of the irreversibility that cannot be reduced due to the component's economic, technological and manufacturing limitations. On the contrary, the avoidable exergy destruction ($\dot{E}x_{D,k}^{AV}$) is a recoverable part of the irreversibility that design modifications and optimisation can reduce.

Four categories for the exergy destruction of the kth components were considered unavoidable-endogenous, unavoidable-exogenous, avoidable-endogenous, and avoidable-exogenous components. The way of component exergy splitting connection is shown in Figure 4 and Equation (31) [19].

$$\dot{E}x_{D,k} = \dot{E}x_{D,k}^{UNEX} + \dot{E}x_{D,k}^{UNEN} + \dot{E}x_{D,k}^{AVEX} + \dot{E}x_{D,k}^{AVEN} \tag{31}$$
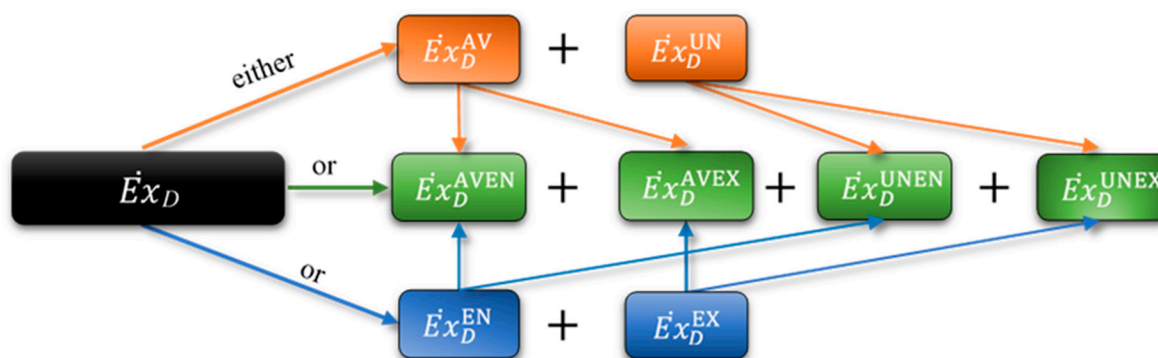

Figure 4. Exergy destruction splitting within a component for advanced exergy analysis.

The value of the unavoidable-exogenous, unavoidable-endogenous, avoidable-exogenous, and avoidable-endogenous exergy destruction for the kth component is calculated as indicated in Equations (32)–(35) [19].

$$\dot{Ex}_{D,k}^{UNEN} = \left(\frac{\dot{Ex}_{D,k}}{\dot{Ex}_{P,k}}\right)^{UN} \dot{Ex}_{P,k}^{EN} \tag{32}$$

$$\dot{Ex}_{D,k}^{UNEX} = \dot{Ex}_{D,k}^{UN} - \dot{Ex}_{D,k}^{UNEN} \tag{33}$$

$$\dot{Ex}_{D,k}^{AVEX} = \dot{Ex}_{D,k}^{EX} - \dot{Ex}_{D,k}^{UNEX} \tag{34}$$

$$\dot{Ex}_{D,k}^{AVEN} = \dot{Ex}_{D,k}^{EN} - \dot{Ex}_{D,k}^{UNEN} \tag{35}$$

3.3.6. Advanced Exergoeconomic Analysis

The advanced exergoeconomic analysis splits components of investment and exergy destruction costs into two unavoidable/avoidable and exogenous/endogenous parts; the combinations of component exergy cost splitting with the component cost are shown in Figure 5 [14].

The costs of the endogenous part of the exergy destruction and investment related to each component are expressed as indicated in Equations (36) and (37) [46].

$$\dot{C}_D^{EN} = c_f \, \dot{Ex}_D^{EN} \tag{36}$$

$$\dot{Z}_k^{EN} = \dot{Ex}_{P,k}^{EN} \left(\frac{\dot{Z}_k}{\dot{Ex}_{P,k}}\right)^{real} \tag{37}$$

In the same way, the cost of the exogenous part is presented in Equations (38) and (39).

$$\dot{C}_D^{EX} = c_f \, \dot{Ex}_D^{EX} \tag{38}$$

$$\dot{Z}_k^{EX} = \dot{Z}_k - \dot{Z}_k^{EN} \tag{39}$$

According to [46], the costs of the unavoidable part of the exergy destruction and investment related to each component that cannot be reduced due to the component's economic and manufacturing methods limitations can be calculated by Equations (40) and (41).

$$\dot{C}_D^{UN} = c_f \, \dot{Ex}_D^{UN} \tag{40}$$

$$\dot{Z}_k^{UN} = \dot{Ex}_{P,k} \left(\frac{\dot{Z}_k}{\dot{Ex}_{P,k}}\right)^{UN} \tag{41}$$

Likewise, the costs of the recoverable part are expressed as follows by Equations (42) and (43).

$$\dot{C}_D^{AV} = c_f \, \dot{Ex}_D^{AV} \tag{42}$$

$$\dot{Z}_k^{AV} = \dot{Z}_k - \dot{Z}_k^{UN} \tag{43}$$

The costs of the unavoidable-endogenous part of the exergy destruction and investment related to each component (cannot be reduced due to the component's economic and manufacturing methods limitations) can be obtained by Equations (44) and (45).

$$\dot{C}_D^{UNEN} = c_f \, \dot{Ex}_D^{UNEN} \tag{44}$$

$$\dot{Z}_k^{UNEN} = \dot{Ex}_{P,k}^{EN} \left(\frac{\dot{Z}_k}{\dot{Ex}_{P,k}}\right)^{UN} \tag{45}$$

Besides, the costs of the unavoidable-exogenous part of the exergy destruction and investment related to each component (can be reduced by improving the performance of the rest component) can be calculated by Equations (46) and (47).

$$\dot{C}_D^{UNEX} = c_f \, \dot{E}x_D^{UNEX} \tag{46}$$

$$\dot{Z}_k^{UNEX} = \dot{Z}_k^{UN} - \dot{Z}_k^{UNEN} \tag{47}$$

Similarly, the costs of the avoidable-endogenous part of the exergy destruction and investment related to each component (can be reduced by improving the performance of the investigated component) are expressed by Equations (48) and (49).

$$\dot{C}_D^{AVEN} = c_f \, \dot{E}x_D^{AVEN} \tag{48}$$

$$\dot{Z}_k^{AVEN} = \dot{Z}_k^{EN} - \dot{Z}_k^{UNEN} \tag{49}$$

In the same way, the costs of the avoidable-exogenous part of the exergy destruction and investment related to each component (can be reduced by improving the performance of the rest component) are computed by Equations (50) and (51).

$$\dot{C}_D^{AVEX} = c_f \, \dot{E}x_D^{AVEX} \tag{50}$$

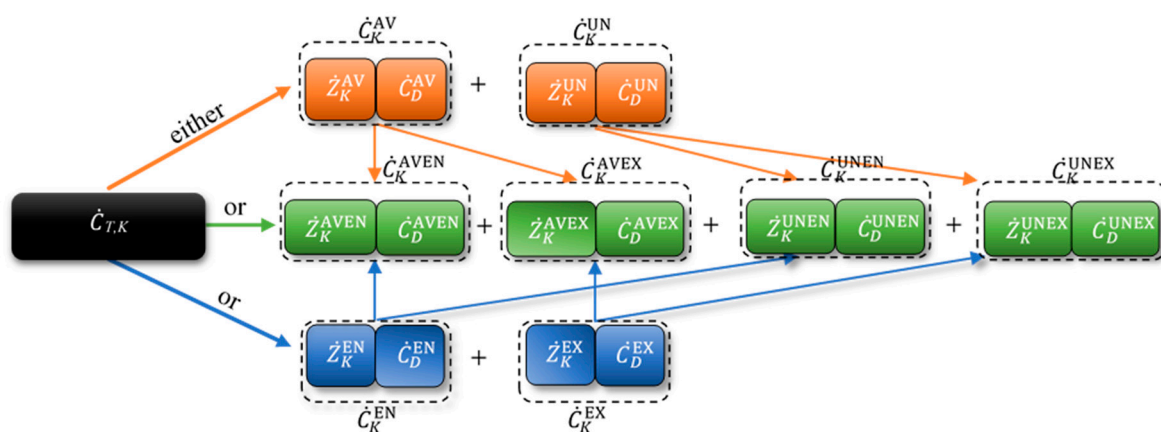$$\dot{Z}_k^{AVEX} = \dot{Z}_k^{EX} - \dot{Z}_k^{UNEX} \tag{51}$$

Figure 5. Advanced exergoeconomic analysis splitting.

4. Results and Discussion

4.1. Conventional Exergoeconomic Analysis

This section analyses the system exergy performance with fixed condensing and evaporating temperatures, and solar intensity, Figure 6a. It states that the compressor represents the largest source of exergy destruction of the whole system's exergy destruction condenser and then ejector. On the other hand, the generator presents the lowest exergy destruction source.

Figure 6b quantifies in detail the percentage of exergy destruction, compressor, 26%, followed by the condenser, 24%, and ejector exergy destruction represents 18% of the total system exergy destruction, which should be further investigated for accounting the source of irreversibility to improve in future designs. Meanwhile, both the second expansion valve and generator comprise the lowest exergy destruction percentage, 3% and 2%, respectively.

(**a**)   (**b**)
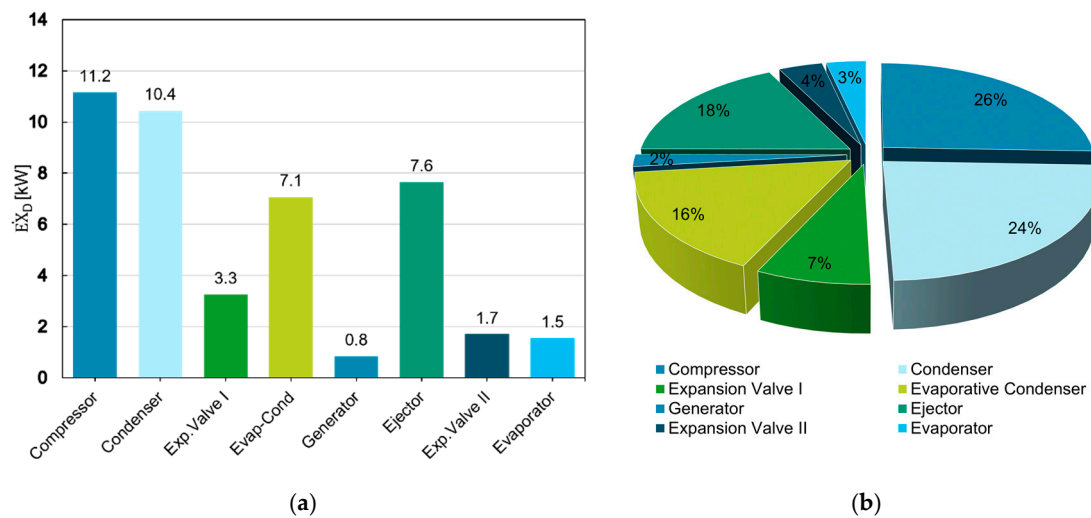
Figure 6. Exergy destruction (**a**) for system component and (**b**) component percentage exergy destruction.

Then, the highest investment cost was for the condenser, followed by the generator, the evaporator, the compressor, and the evaporative condenser. According to the investment costs, the second expansion valve and the ejector have the lost system components cost, Table 6.

On the other side, the compressor represents the highest cost of exergy destructions, followed by the ejector and condenser, whilst the second expansion valve had the lowest destruction costs in the system. The conventional exergoeconomic analysis showed that the second expansion valve and the generator were not significant system components concerning lowering the costs. In contrast, the compressor, the ejector, and the condenser were essential components.

Table 6. Results of conventional exergoeconomic analysis.

Components	$\dot{C}_D$ [$ h⁻¹]	Z_K [$ h⁻¹]	Z_{OM} [$ h⁻¹]	Z_{CL} [$ h⁻¹]
Compressor	18.448	4.340	2.230	2.110
Condenser	5.034	20.950	10.780	10.170
Evaporative-Condenser	3.455	1.100	0.570	0.530
Expansion Valve I	0.991	0.009	0.005	0.005
Generator	0.412	13.920	7.160	6.760
Ejector	6.969	0.001	0	0
Expansion Valve II	0.261	0.004	0.002	0.002
Evaporator	0.649	9.77	5.03	4.74
Total	36.22	50.12	25.79	24.33

4.2. Advanced Exergy Analysis

The advanced exergy analysis results are summarised in Table 7. As a result of the endogenous exergy destruction evaluation, the condenser has the more significant exergy destruction (9.407 kW, 22% of the total) followed by evaporative-condenser (6.685 kW, 15%), and compressor (1.943 kW, 4%), meanwhile the second expansion valve represent the lowest endogenous exergy destruction of (0.4435 kW, 1%). Besides, the exogenous exergy destruction evaluation result shows that the compressor represents the highest source of exergy destruction (9.218 kW, 21% of total system exergy destruction). In comparison, the evaporator represents the lowest (0.0334 kW, 0.08%). Meanwhile, the total system endogenous exergy destruction and exogenous exergy destruction represent 53% and 47% of the total system exergy destruction, respectively. This indicates that these components' exergy destruction is mainly due to their irreversible losses rather than the rest

of the components associated with them. Therefore, priority should be given to improve each component when system optimisation is carried out. This also implies that the influence of the interactions between components is not very strong.

On the other hand, from the avoidable-unavoidable exergy destruction evaluation, the compressor represents the highest source of irreversibility, 21% of the whole system thermodynamic inefficiencies that can be avoided by further design, followed by ejector and condenser, 17% and 8%, respectively.

Finally, by combining the two splitting approaches, the results of this combination show that the avoidable exogenous part represents the highest exergy destruction, 37% of the total system exergy destruction, Figure 7. Hence, the compressor represents the highest source of avoidable exogenous destruction (9.176 kW, 21% of the total system exergy destruction), followed by the ejector (6.013 kW, 14%). Meanwhile, the unavoidable endogenous part represents the second-highest exergy destruction, 33% of total system exergy destruction (Figure 7). Hence, the condenser represents the highest source of the unavoidable endogenous part (6.3 kW, 14% of total system exergy destruction). On the other hand, the evaporator represents the lowest source of unavoidable exergy destruction. Figure 8 shows the exergy flow for the proposed system; the compressor, condenser, and ejector represent the highest avoidable exergy destruction parts for the whole system. It should give more attention by improving these components; the exergy destruction in these components can effectively decrease, leading to increased overall system COP and exergy efficiency.

Table 7. Advanced exergy analysis of the main system components.

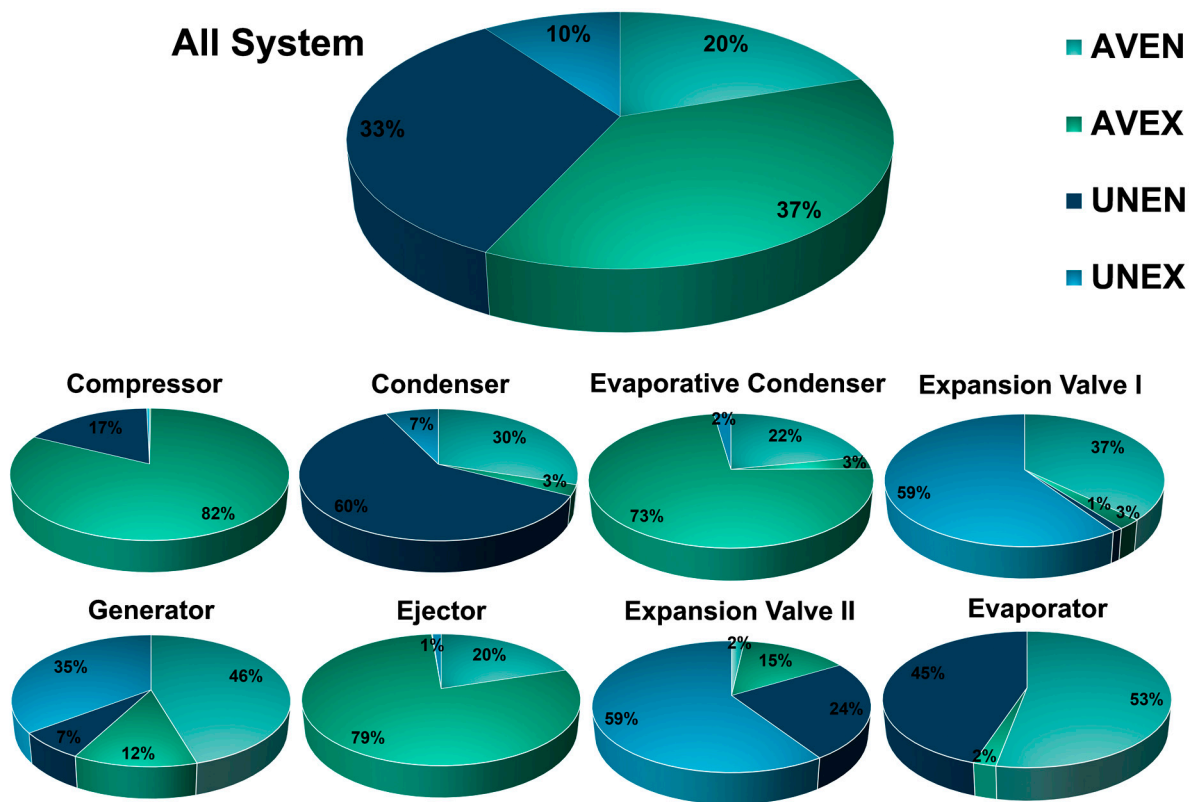| Components	$\dot{EX}_D$ [kW]	$\dot{EX}_D^{EN}$ [kW]	$\dot{EX}_D^{EX}$ [kW]	$\dot{EX}_D^{UN}$ [kW]	$\dot{EX}_D^{AV}$ [kW]	$\dot{EX}_D^{UNEN}$ [kW]	$\dot{EX}_D^{UNEX}$ [kW]	$\dot{EX}_D^{AVEN}$ [kW]	$\dot{EX}_D^{AVEX}$ [kW]
Compressor	11.16	1.94	9.22	9.19	1.97	1.93	0.04	0.02	9.18
	26%	4%	21%	21%	5%	4%	0%	0%	21%
Condenser	10.44	9.41	1.03	3.40	7.04	6.29	0.75	3.12	0.28
	24%	22%	2%	8%	16%	14%	2%	7%	1%
Evap-Condenser	7.07	6.69	0.38	1.76	5.31	5.15	0.16	1.54	0.22
	16%	15%	1%	4%	12%	12%	0%	4%	1%
Generator	0.84	0.44	0.40	0.49	0.36	0.06	0.30	0.38	0.10
	2%	1%	1%	1%	1%	0%	1%	1%	0%
Ejector	7.65	1.54	6.10	7.55	0.10	0.01	0.09	1.53	6.01
	18%	4%	14%	17%	0%	0%	0%	4%	14%
Exp. Valve I	3.25	1.24	2.01	1.29	1.96	0.03	1.93	1.21	0.08
	7%	3%	5%	3%	5%	0%	4%	3%	0%
Exp. Valve II	1.70	0.44	1.25	1.42	0.28	0.41	1.00	0.03	0.25
	4%	1%	3%	3%	1%	1%	2%	0%	1%
Evaporator	1.54	1.50	0.03	0.85	0.69	0.69	0.00	0.81	0.03
	4%	3%	0%	2%	2%	2%	0%	2%	0%
Total Exergy	43.64	23.21	20.43	17.70	25.93	14.56	4.28	8.65	16.15
	100%	53%	47%	40.6%	59.4%	33%	10%	20%	37%

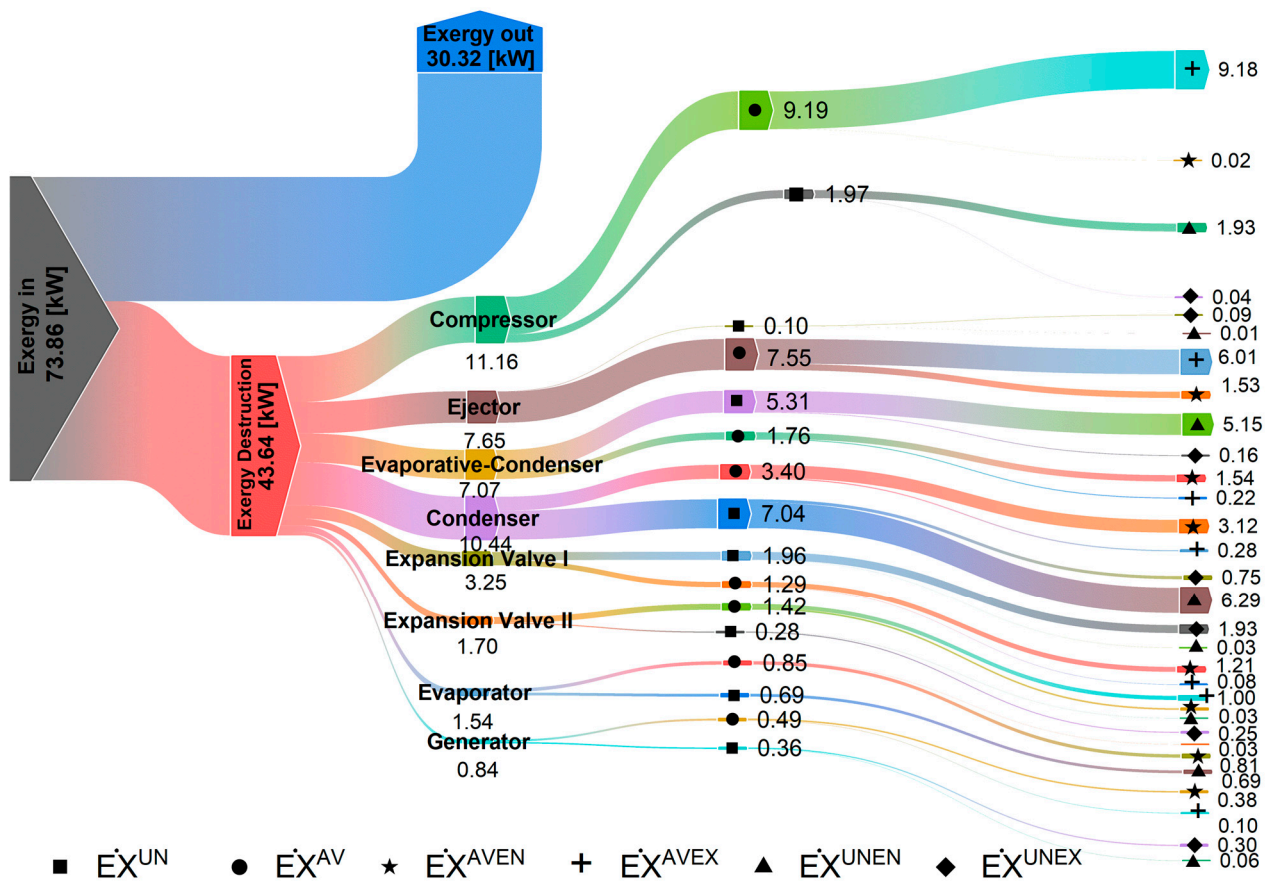**Figure 7.** Percentage exergy destruction rate of system components.

Figure 8. Sankey diagram of exergy flow.

4.3. Sensitivity Analysis

To better understand the components' internal condition influences on exergy destruction, a sensitive analysis study is adopted by varying each component's operating characteristic, setting the others. This section focuses on system avoidable exergy destruction sources because it represents a potential for improvement. According to the above previous exergy analysis, all compressors, condensers, and ejectors possess the highest performance improvement priority (represent the highest source of avoidable exergy destruction Figure 8). So that the study focused on these components only, the rest of the components were excluded.

Figure 9 illustrates the effect of compressor efficiency variation on the exogenous exergy destruction of system components. The compressor exogenous exergy destruction shows a remarkable reduction with compressor efficiency increasing. Besides, none of the other components show any influences with compressor efficiency variation, just a slight reduction with condenser due to the corresponding decrease in the condenser inlet temperature (Figure 9c).

Figure 9b evidence that the compressor avoidable exogenous exergy destruction is inversely proportional to the compressor efficiency. Meanwhile, the compressor total and system exergy destruction decrease with a compressor efficiency increase; this enhances compressor consumption power (Figure 9c) to system exergy efficiency and COP (Figure 9d), owing to compressor irreversibility and system reduction.
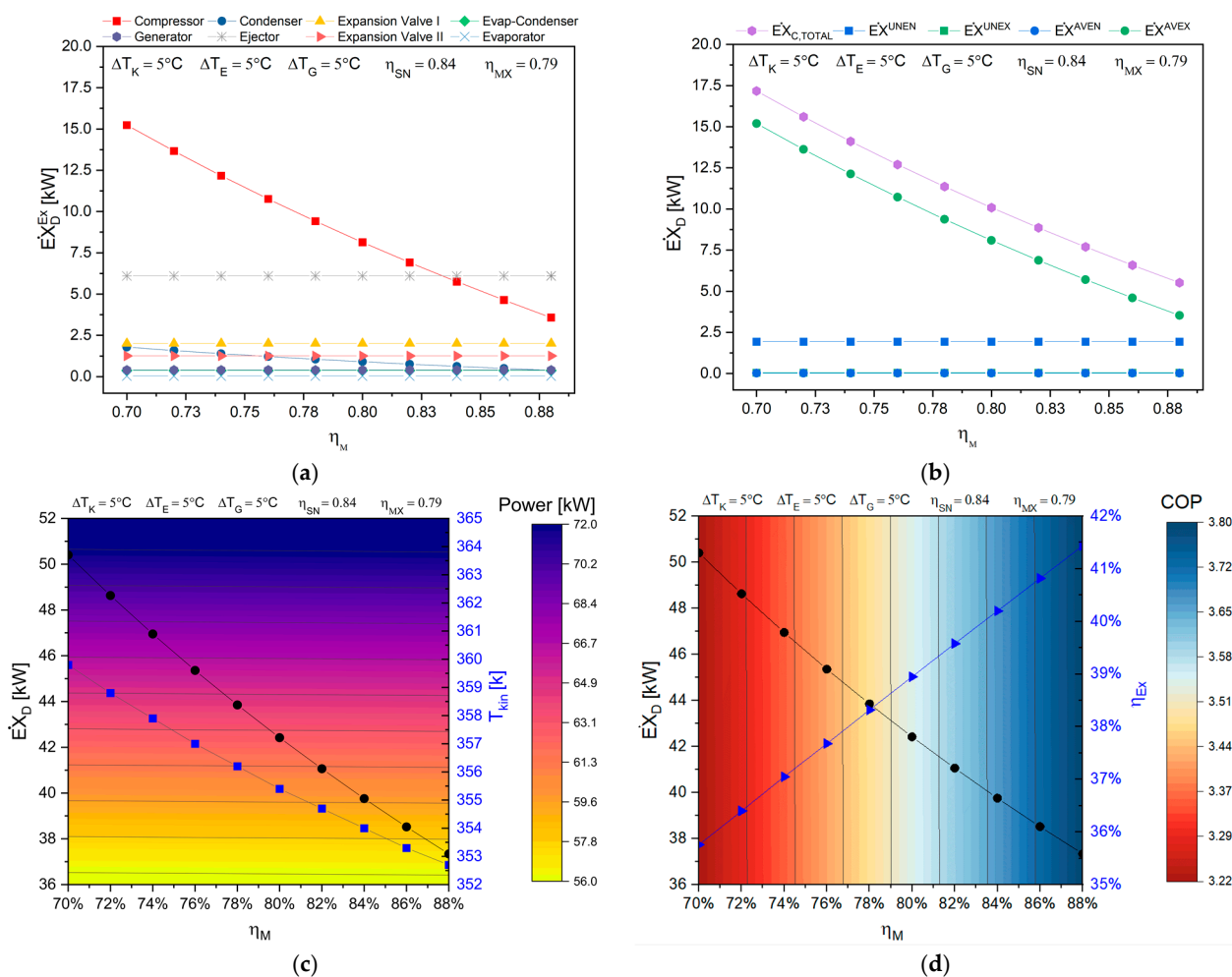
Figure 9. Compressor efficiency variation influence: (**a**) components exergy exogenous part, (**b**) compressor exergy destruction parts, (**c**) consumption power, and (**d**) system COP-exergy efficiency.

Figure 10 shows the effect of condenser glide temperature variation on system components exogenous exergy destruction. The condenser exogenous exergy destruction increases with higher glide temperature due to condenser temperature augmentation. Meanwhile, the other components are slightly increased with glide temperature variation. At constant inlet and outlet conditions of condenser cooling water, this causes the heat transfer between the condenser and its condensing medium to decrease and increase the cycle's irreversibility.

Figure 10b shows the influence of condenser glide temperature variations on the condenser exergy destruction. The avoidable exogenous part of condenser exergy destruction is directly proportional with condenser glide temperature increasing; meanwhile, none of the other parts is influenced. Additionally, condenser glide temperature increase has the worst effect on compressor power (Figure 10c), system exergy efficiency and system COP. As a result, the overall system exergy destruction increases at a higher condenser glide temperature (Figure 10d).
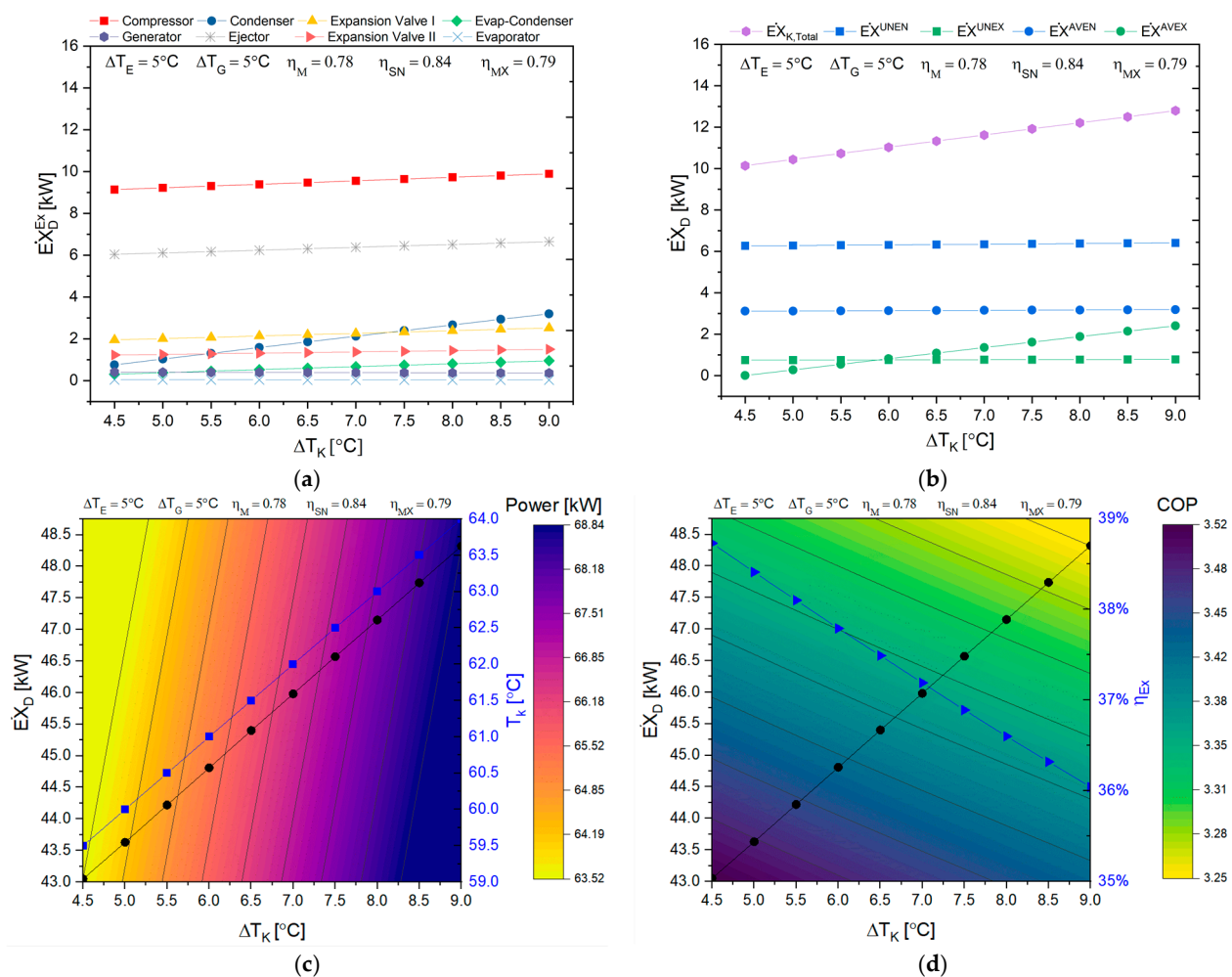
Figure 10. Condenser glide temperature variation influence: (**a**) components exergy exogenous part, (**b**) ejector exergy destruction parts, (**c**) refrigerant mass flow rate, and (**d**) system COP-exergy.

Finally, Figure 11a illustrates the influence of ejector efficiency variation on system components exogenous exergy destruction. The ejector efficiency increasing diminishes the ejector exogenous exergy destruction. Meanwhile, the rest of the components have a negligible variation. The ejector has varied irreversibility sources, such as the nozzles flow friction irreversibility, two streams mixing irreversibility (primary and secondary flow), and compression shock waves irreversibility [47].

On the other hand, Figure 11b shows the influences of ejector efficiency variations on the ejector exergy destruction. The avoidable exogenous part of ejector exergy destruction decreases with ejector efficiency increasing; meanwhile, it shows a lower influence on the rest of the ejector exergy destruction. An ejector efficiency increase enhances condenser heat capacity due to a higher refrigerant mass flow rate (Figure 11c). Meanwhile, despite the overall exergy destruction increase, both the system exergy efficiency and COP are less enhanced, increasing ejector efficiency. The overall system exergy developed increasing; the factor takes a dominant role Figure 11d, attributed to overall system mass flow rate increases.
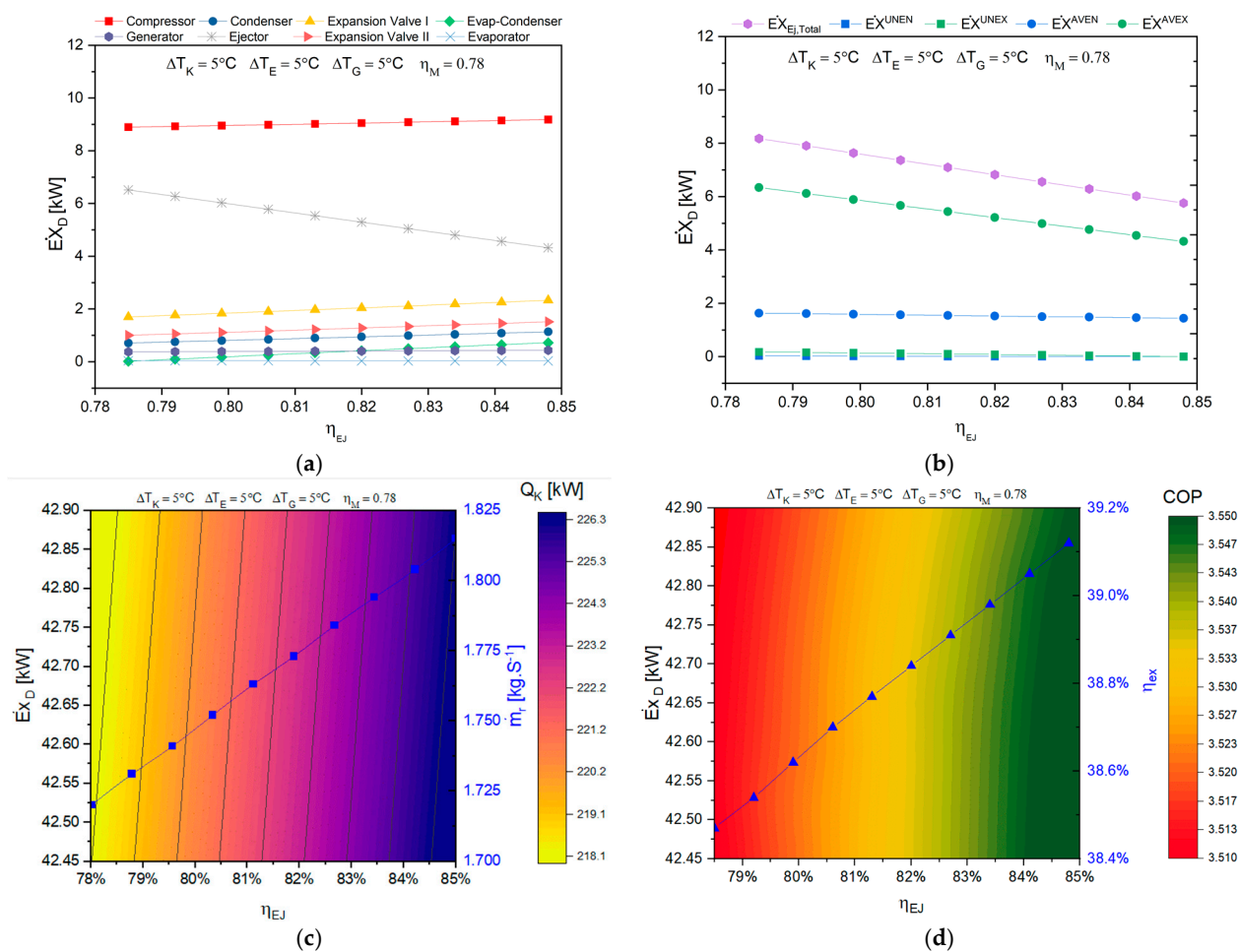
Figure 11. Ejector efficiency variation influence: (**a**) components exergy exogenous part, (**b**) ejector exergy destruction parts, (**c**) refrigerant mass flow rate, and (**d**) system COP-exergy efficiency.

### 4.4. Advanced Exergoeconomic Analysis

From the advanced exogenous analysis, Table 8, a significant proportion of investment destruction costs in the system are detected as exogenous (71%). Meanwhile, the avoidable destruction cost represents 62% of the overall destruction costs and avoidable-exogenous cost, 58%. In contrast, unavoidable-exogenous destruction cost was relatively low.

The highest exergy destruction costs are accumulated in the compressor, 41.9% of the total exergy destruction in avoidable exogenous. The generator follows it. A substantial proportion of the exergy destruction cost is avoidable-exogenous, 15.1% of the overall system investment costs (approximately 79% of the generator exergy destruction cost, Figure 12). The third significant exergy destruction cost is accumulated in a condenser. Still, in this case, it is unavoidable-endogenous, 8.4% of the overall system investment costs (approximately 60% of the condenser exergy destruction cost, Figure 12). The two parts of

avoidable exergy cost (AVEN and AVEX) components are 3.9% and 0.2% of overall system investment costs. Consequently, the second expansion valve exergy destruction costs represent a narrow share of the destruction costs (0.7%). Therefore, improvements concentrated on the second expansion valve destructions would have limited importance and investment costs.

Table 8. Exergy destruction cost rate of each system component.

Components	$\dot{C}_D$ [\$ h⁻¹]	$\dot{C}_D^{EN}$ [\$ h⁻¹]	$\dot{C}_D^{EX}$ [\$ h⁻¹]	$\dot{C}_D^{UN}$ [\$ h⁻¹]	$\dot{C}_D^{AV}$ [\$ h⁻¹]	$\dot{C}_D^{UNEN}$ [\$ h⁻¹]	$\dot{C}_D^{UNEX}$ [\$ h⁻¹]	$\dot{C}_D^{AVEN}$ [\$ h⁻¹]	$\dot{C}_D^{AVEX}$ [\$ h⁻¹]
Compressor	18.45	3.25	15.20	3.21	15.24	3.18	0.07	0.03	15.17
	50.9%	9.0%	42.0%	8.9%	42.1%	8.8%	0.2%	0.1%	41.9%
Condenser	5.03	3.39	1.64	4.54	0.50	3.03	0.36	1.50	0.13
	13.9%	9.4%	4.5%	12.5%	1.4%	8.4%	1.0%	4.2%	0.4%
Evap-Condenser	3.45	2.60	0.86	3.27	0.19	2.52	0.08	0.75	0.11
	9.5%	7.2%	2.4%	9.0%	0.5%	6.9%	0.2%	2.1%	0.3%
Expansion Valve I	0.41	0.17	0.24	0.22	0.20	0.03	0.15	0.19	0.05
	1.1%	0.5%	0.7%	0.6%	0.5%	0.1%	0.4%	0.5%	0.1%
Generator	6.97	0.09	6.88	1.41	5.56	0.01	0.08	1.40	5.48
	19.2%	0.3%	19.0%	3.9%	15.4%	0%	0.2%	3.9%	15.1%
Ejector	0.99	0.60	0.39	0.38	0.61	0.01	0.59	0.37	0.02
	2.7%	1.7%	1.1%	1.0%	1.7%	0.0%	1.6%	1.0%	0.1%
Expansion Valve II	0.26	0.04	0.22	0.07	0.19	0.06	0.15	0	0.04
	0.7%	0.1%	0.6%	0.2%	0.5%	0.2%	0.4%	0%	0.1%
Evaporator	0.65	0.29	0.36	0.63	0.01	0.29	0.00	0.34	0.01
	1.8%	0.8%	1.0%	1.8%	0%	0.8%	0%	0.9%	0%
Total	36.22	10.44	25.78	13.72	22.50	9.13	1.48	4.59	21.01
	100%	29%	71%	38%	62%	25%	4%	13%	58%
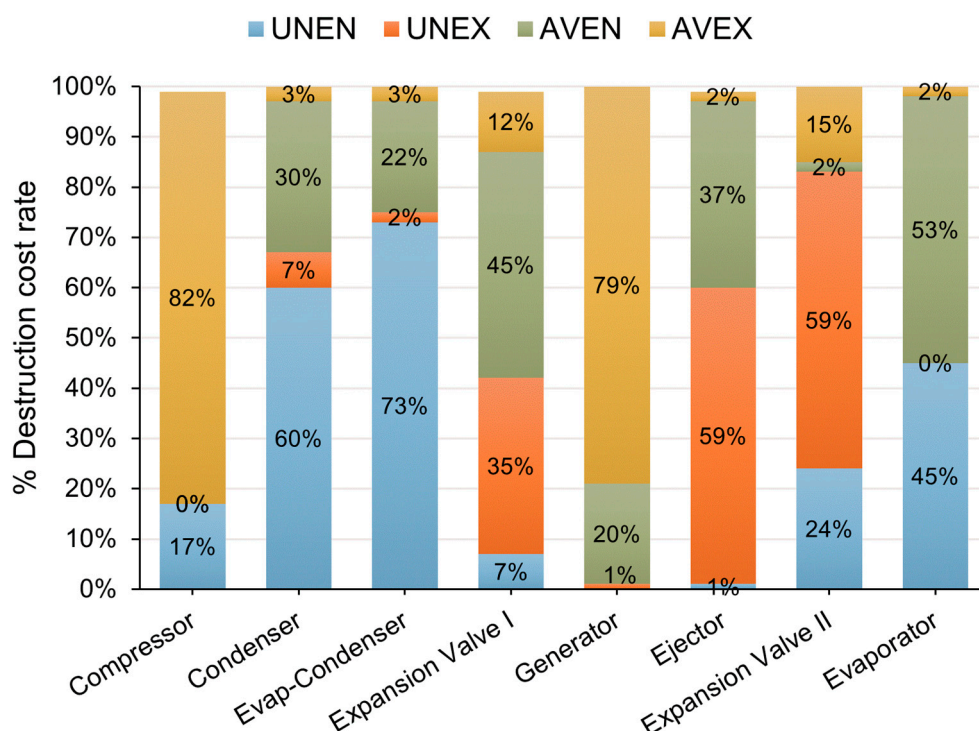
Figure 12. Breakdown of percentage advanced exergy destruction cost rate of the main components.

From Table 9, 51% of the system costs are unavoidable; meanwhile, 29% is avoidable exogenous and 20% is avoidable endogenous. In system components cost comparison, the highest cost comes from the condenser (30%), followed by the compressor (26.4%) and generator (24%), and both expansion valve represents the lowest components cost (below 1%).

From Figure 13, 68% of compressor cost is avoidable, and according to Table 9, the compressor has an exergoeconomic factor (f) of 19%. It indicates that the exergy destruction cost has a marked influence on total compressor cost; therefore, it should improve the compressor performance. For the generator, 43% of the investigated cost is avoidable with an exergoeconomic factor of 67%; this indicates that the construction cost significantly influences total generator cost. The same conclusion as the compressor can be drafted.

In the same context, the ejector has the lowest exergoeconomic factor (0.1%), and it should be getting more attention to reduce the irreversibility by design improvement. On the contrary, the evaporator has the highest exergoeconomic factor (94%), giving more about evaporator construction for improving.

On the other hand, approximately half of the total investment costs (49%) were avoidable, and 29% of the system exergy destruction is exogenous avoidable, larger than endogenous avoidable exergy destruction. It indicates that the interaction between components is strong, and the exergy destruction of these components are mainly due to irreversible losses of components associated with them.

Table 9. Investment cost rate of the system components.

| Components	$\dot{Z}_T$ [\$ h⁻¹]	$\dot{Z}_T^{EN}$ [\$ h⁻¹]	$\dot{Z}_T^{EX}$ [\$ h⁻¹]	$\dot{Z}_T^{UN}$ [\$ h⁻¹]	$\dot{Z}_T^{AV}$ [\$ h⁻¹]	$\dot{Z}_T^{UNEN}$ [\$ h⁻¹]	$\dot{Z}_T^{UNEX}$ [\$ h⁻¹]	$\dot{Z}_T^{AVEN}$ [\$ h⁻¹]	$\dot{Z}_T^{AVEX}$ [\$ h⁻¹]	f
Compressor	22.79	7.02	15.78	7.27	15.52	6.91	0.15	0.33	15.41	19%
	26.4%	8.1%	18.3%	8.4%	18.0%	8.0%	0.2%	0.4%	17.9%	
Condenser	25.98	20.76	5.23	21.47	4.51	17.02	2.59	5.59	0.78	81%
	30%	24%	6%	25%	5%	20%	3%	6%	1%	
Evap- Condenser	4.56	4.26	0.29	3.05	1.51	2.93	0.66	0.80	0.17	24%
	5.3%	4.9%	0.3%	3.5%	1.7%	3.4%	0.8%	0.9%	0.2%	
Expansion Valve I	0.42	0.22	0.20	0.18	0.24	0.03	0.15	0.19	0.05	2%
	0.5%	0.3%	0.2%	0.2%	0.3%	0.0%	0.2%	0.2%	0.1%	
Generator	20.89	11.86	9.03	1.18	19.71	0.97	9.57	1.53	8.82	67%
	24%	14%	10%	1%	23%	1%	11%	2%	10%	
Ejector	0.99	0.38	0.61	0.60	0.39	0.01	0.59	0.37	0.02	0.1%
	1.1%	0.4%	0.7%	0.7%	0.5%	0.0%	0.7%	0.4%	0.0%	
Expansion Valve II	0.27	0.07	0.19	0.04	0.22	0.07	0.16	0.01	0.04	2%
	0.3%	0.1%	0.2%	0.1%	0.3%	0.1%	0.2%	0.0%	0.0%	
Evaporator	10.42	2.47	7.95	10.06	0.36	2.12	0.00	8.28	0.01	94%
	12.1%	2.9%	9.2%	11.7%	0.4%	2.5%	0.0%	9.6%	0.0%	
Total	86.31	47.04	39.28	43.86	42.46	30.05	13.87	17.07	25.31	
	100%	54%	46%	51%	49%	35%	16%	20%	29%	
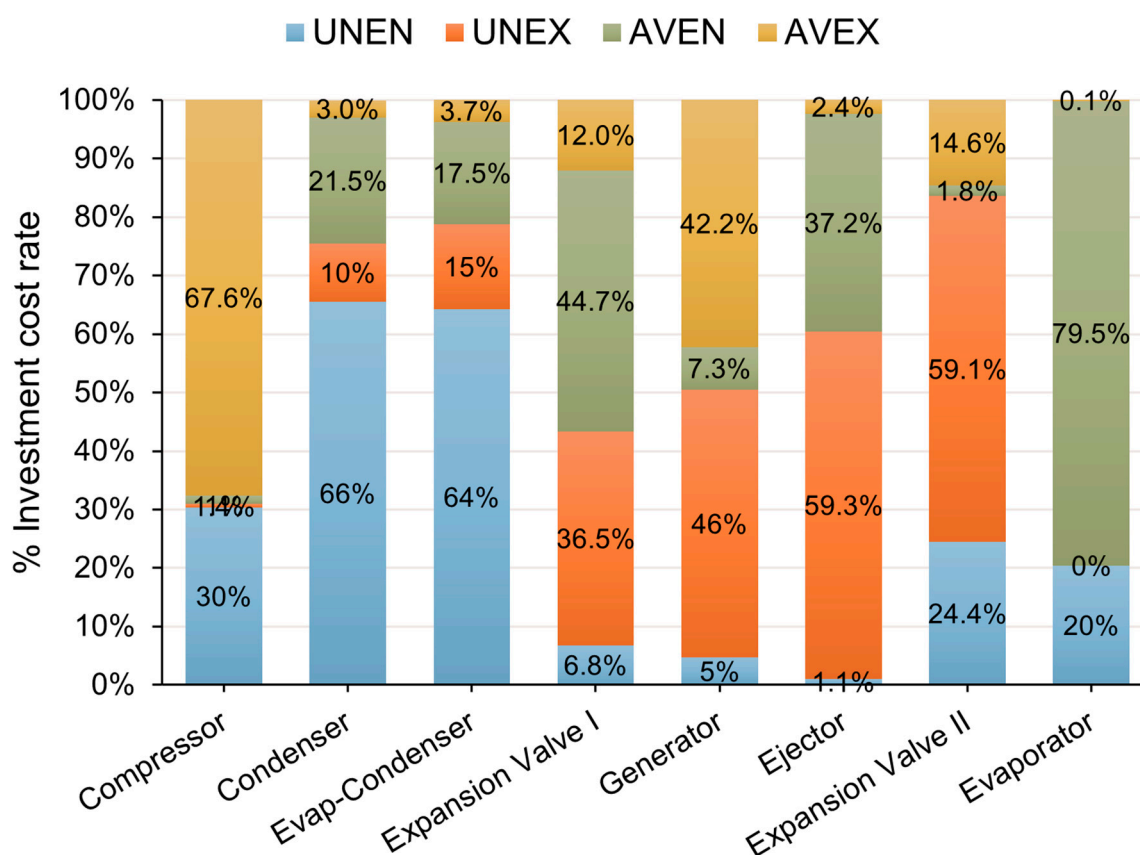
Figure 13. Percentage of components cost rate.

5. Conclusions

Conventional and advanced exergoeconomic analyses are performed to compound the ejector-heat pump for simultaneous data centre cooling and district heating. The conclusions obtained from the current study are summarised as follows.

- The compressor represents the largest exergy destruction source of the whole system, with 26% coming from the conventional exergy analysis, followed by the condenser ejector, 24% and 18%. On the other hand, the generator shows the lowest exergy destruction source, 2%.
- Moreover, the advanced exergy analysis indicates that 59.4% of the whole system exergy destruction can be avoided by further design optimisation. Among them, reducing the refrigerant side pressure drop across the heat exchangers by rearranging refrigerant circuiting [48], decreasing the amount of flashing gas at the evaporator inlet by nozzle [49], or by using a flash tank with a vapour injection scroll compressor [50], and reducing the pressure drop in the suction nozzle. The compressor contributes the highest share (21%) of the exergy destruction rate in an avoidable exogenous form, followed by the ejector (14%) and condenser (7%).
- The quantitative analysis suggests that the compressor efficiency increase positively influences the system COP by reducing the consumption power. The compressor efficiency increase has a reduced effect on compressor avoidable exogenous exergy destruction and total system exergy destruction. In the same context, condenser glide temperature increasing has the worst effect on the avoidable exogenous part of condenser exergy destruction, system exergy performance and system COP. Finally, the ejector efficiency increase slightly enhances the system COP, as does the avoidable exogenous part of ejector exergy destruction.
- The condenser represents the highest cost for the system economic comparison, followed by the compressor and generator (30%, 26.4%, and 24%), and both expansion

valves represent the lowest components cost (lower than 1%). Moreover, the advanced exergoeconomic results show that 51% of the system costs are unavoidable.

- The ejector has the lowest exergoeconomic factor, 0.1%, and it should be getting more attention to reduce the irreversibility by design improvement. On the contrary, the evaporator has the highest exergoeconomic factor, 94%, and its construction is quite relevant.

Author Contributions: A.K.S.A.-S.: Conceptualisation, methodology, software writing—original draft, writing—review & editing. A.M.-B.: Conceptualisation, methodology, writing—review & editing, resources, supervision. J.N.-E.: writing—review & editing, supervision, project administration, funding acquisition. V.M.S.-F.: review & editing. All authors have read and agreed to the published version of the manuscript.

Conflicts of Interest: The authors declare there is no conflict of interest.

Nomenclature

COP	Coefficient of performance (-)
$\dot{C}$	Cost rate ($ h^{-1})
D	Diameter (mm)
EER	Energy efficiency ratio (-)
$\dot{EX}$	Exergy rate (kJ s^{-1})
h	Specific enthalpy (kJ kg^{-1})
f	Exergoeconomic factor
I	Solar intensity (W m^{-2})
NBP	Normal boiling point (°C)
P	Pressure (MPa)
rpm	Revolution per minute
T	Temperature (°C)
V	Volume (m^3)
$\dot{m}$	Refrigerant mass flow rate (kg s^{-1})
$\dot{Q}$	Heat transfer rate (kW)
$\dot{W}$	Electrical consumption power (kW)
Z	Capital cost function ($)

Greek symbols

α	System operational lifetime (year)
ε	Heat exchanger effectiveness (-)
v	Specific volume (m^3 kg^{-1})
η	Efficiency (-)
μ	Entrainment ratio (-)
ω	Refrigerant velocity (m s^{-1})
φ	Maintenance factor

Superscripts

AV	Avoidable
UN	Unavoidable
EX	exogenous
EN	endogenous

Subscripts

C	Compressor
CM	Capital and maintenance

Cri	Critical condition
D	Diffuser, discharge, destruction
Ds	Displacement
e	Evaporator
ea	Actual exit condition
ej	Ejector
ek	Evaporative-condenser
em	Electrical mechanical
es	Isentropic exit condition
EW	Evaporator cooling water
exp	Expansion valve
F	Fuel
fg	vaporisation
G	Generator
h	Hot stream
HX	Heat exchanger
in	Inlet
IR	Interest rate
is	Isentropic conditions
k	Condenser, component
kw	Condenser cooling water
l	Cold stream
mx	Mixing conditions
n	Normal shock conditions
OP	Operating
out	Outlet
p	Primary stream
pn	Primary nozzle
r	Refrigerant
s	Secondary stream, Suction
sn	Suction nozzle
t	Total
v	Volumetric
w	Water stream

Abbreviatures

ASHRAE	The American Society of Heating, Refrigerating and Air-Conditioning
EES	Engineering Equation Solver
Evap	Evaporative
HP	Heat Pump
ICT	The Information and Communications Technology
PV/T	Photovoltaic Thermal

References

1. OECD/IEA. World Energy Outlook 2018. Available online: https://iea.blob.core.windows.net/assets/77ecf96c-5f4b-4d0d-9d93-d81b938217cb/World_Energy_Outlook_2018.pdf (accessed 2 February 2021).
2. IEA. World Energy Outlook 2019. Available online: https://iea.blob.core.windows.net/assets/98909c1b-aabc-4797-9926-35307b418cdb/WEO2019-free.pdf (2 February 2021).
3. European Commission Ecodesign Preparatory Study on Enterprise Servers and Data Equipment. 2015; ISBN 9789279519345.Available online: https://op.europa.eu/en/publication-detail/-/publication/6ec8bbe6-b8f7-11e5-8d3c-01aa75ed71a1 (12 February 2021).

4. Avgerinou, M.; Bertoldi, P.; Castellazzi, L. Trends in Data Centre Energy Consumption under the European Code of Conduct for Data Centre Energy Efficiency. *Energ.* **2017**, *10*, doi:10.3390/en10101470.

5. Payerle, G.; Team, R.C.; Sartor, D.; Dolnicar, S.; Chapple, A.; Pastuszak, A.W.; Wang, R. Report to Congress on Server and Data Center Energy Efficiency public law 109-431. Public law 109. *Ann. Tour. Res.* **2015**, *3*, doi:10.2172/929723.

6. IEA The Future of Cooling: Opportunities for energy-efficient air conditioning. *Futur. Cool. Oppor. Energy-Effic. Air Cond.* **2018**, 92.

7. Byrne, P.; Ghoubali, R. Exergy analysis of heat pumps for simultaneous heating and cooling. *Appl. Therm. Eng.* **2019**, *149*, 414–424, doi:10.1016/j.applthermaleng.2018.12.069.

8. Bellos, E.; Tzivanidis, C.; Moschos, K.; Antonopoulos, K.A. Energetic and financial evaluation of solar assisted heat pump space heating systems. *Energy Convers. Manag.* **2016**, *120*, 306–319, doi:10.1016/j.enconman.2016.05.004.

9. Khalid Shaker Al-Sayyab, A.; Mota-Babiloni, A.; Navarro-Esbrí, J. Novel compound waste heat-solar driven ejector-compression heat pump for simultaneous cooling and heating using environmentally friendly refrigerants. *Energy Convers. Manag.* **2021**, *228*, 113703, doi:10.1016/j.enconman.2020.113703.

10. Fu, H.D.; Pei, G.; Ji, J.; Long, H.; Zhang, T.; Chow, T.T. Experimental study of a photovoltaic solar-assisted heat-pump/heat-pipe system. *Appl. Therm. Eng.* **2012**, *40*, 343–350, doi:10.1016/j.applthermaleng.2012.02.036.

11. Zhang, X.; Zhao, X.; Shen, J.; Hu, X.; Liu, X.; Xu, J. Design, fabrication and experimental study of a solar photovoltaic/loop-heat-pipe based heat pump system. *Sol. Energy* **2013**, *97*, 551–568, doi:10.1016/j.solener.2013.09.022.

12. Xu, Y.; Guo, F.; Song, M.; Jiang, N.; Wang, Q.; Chen, G. Exergetic and economic analyses of a novel modified solar-heat-powered ejection-compression refrigeration cycle comparing with conventional cycle. *Energy Convers. Manag.* **2018**, *168*, 107–118, doi:10.1016/j.enconman.2018.04.098.

13. Chen, G.; Ierin, V.; Volovyk, O.; Shestopalov, K. Thermodynamic analysis of ejector cooling cycles with heat-driven feed pumping devices. *Energy* **2019**, *186*, 115892, doi:10.1016/j.energy.2019.115892.

14. Tsatsaronis, G.; Park, M.-H. On avoidable and unavoidable exergy destructions and investment costs in thermal systems. *Energy Convers. Manag.* **2002**, *43*, 1259–1270, doi:10.1016/S0196-8904(02)00012-2.

15. Morosuk, T.; Tsatsaronis, G.; Zhang, C. Conventional thermodynamic and advanced exergetic analysis of a refrigeration machine using a Voorhees' compression process. *Energy Convers. Manag.* **2012**, *60*, 143–151, doi:10.1016/j.enconman.2012.02.021.

16. Singh, A.; Sarkar, J.; Sahoo, R.R. Experimental energy, exergy, economic and exergoeconomic analyses of batch-type solar-assisted heat pump dryer. *Renew. Energy* **2020**, *156*, 1107–1116, doi:10.1016/j.renene.2020.04.100.

17. Morosuk, T.; Tsatsaronis, G. Advanced exergetic evaluation of refrigeration machines using different working fluids. *Energy* **2009**, *34*, 2248–2258, doi:10.1016/j.energy.2009.01.006.

18. Erbay, Z.; Hepbasli, A. Application of conventional and advanced exergy analyses to evaluate the performance of a ground-source heat pump (GSHP) dryer used in food drying. *Energy Convers. Manag.* **2014**, *78*, 499–507, doi:10.1016/j.enconman.2013.11.009.

19. Chen, J.; Havtun, H.; Palm, B. Conventional and advanced exergy analysis of an ejector refrigeration system. *Appl. Energy* **2015**, *144*, 139–151, doi:10.1016/j.apenergy.2015.01.139.

20. Zhao, H.; Yuan, T.; Gao, J.; Wang, X.; Yan, J. Conventional and advanced exergy analysis of parallel and series compression-ejection hybrid refrigeration system for a household refrigerator with R290. *Energy* **2019**, *166*, 845–861, doi:10.1016/j.energy.2018.10.135.

21. Gullo, P. Impact and quantification of various individual thermodynamic improvements for transcritical R744 supermarket refrigeration systems based on advanced exergy analysis. *Energy Convers. Manag.* **2021**, *229*, doi:10.1016/j.enconman.2020.113684.

22. Ambriz-Díaz, V.M.; Rubio-Maya, C.; Ruiz-Casanova, E.; Martínez-Patiño, J.; Pastor-Martínez, E. Advanced exergy and exergoeconomic analysis for a polygeneration plant operating in geothermal cascade. *Energy Convers. Manag.* **2020**, *203*., doi:10.1016/j.enconman.2019.112227.

23. Erbay, Z.; Hepbasli, A. Advanced exergoeconomic evaluation of a heat pump food dryer. *Biosyst. Eng.* **2014**, *124*, 29–39, doi:10.1016/j.biosystemseng.2014.06.008.

24. Klein, S. *Engineering Equation Solver (EES) V10.2*. Fchart software: Madison, USA, 2020.

25. NIST Reference Fluid Thermodynamic and Transport Properties Database (REFPROP) 2018.

26. SOLARGIS. Global Solar Atlas. Available online: https://globalsolaratlas.info/ (accessed on 12 January 2021).

27. Sahoo, P.K. Exergoeconomic analysis and optimisation of a cogeneration system using evolutionary programming. *Appl. Therm. Eng.* **2008**, *28*, 1580–1588, doi:10.1016/j.applthermaleng.2007.10.011.

28. Chen, J.; Yu, J. Theoretical analysis on a new direct expansion solar assisted ejector-compression heat pump cycle for water heater. *Sol. Energy* **2017**, *142*, 299–307, doi:10.1016/j.solener.2016.12.043.

29. Bai, T.; Yan, G.; Yu, J. Thermodynamic assessment of a condenser outlet split ejector-based high temperature heat pump cycle using various low GWP refrigerants. *Energy* **2019**, *179*, 850–862, doi:10.1016/j.energy.2019.04.191.

30. Cui, Z.; Qian, S.; Yu, J. Performance assessment of an ejector enhanced dual temperature refrigeration cycle for domestic refrigerator application. *Appl. Therm. Eng.* **2020**, *168*, doi:10.1016/j.applthermaleng.2019.114826.

31. Pan, M.; Bian, X.; Zhu, Y.; Liang, Y.; Lu, F.; Xiao, G. Thermodynamic analysis of a combined supercritical CO2 and ejector expansion refrigeration cycle for engine waste heat recovery. *Energy Convers. Manag.* **2020**, *224*, doi:10.1016/j.enconman.2020.113373.

32. Bejan, A.; Tsatsaronis, G.; Moran, M.J. *Thermal Design and Optimisation*; John Wiley & Sons: Haboken, NJ, USA, 1995; ISBN 0471584673.
33. Roy, R.; Mandal, B.K. Thermo-economic Assessment and Multi-Objective Optimisation of Vapour Compression Refrigeration System using Low GWP Refrigerants. In Proceedings of the 8th International Conference on Modeling Simulation and Applied Optimization (ICMSAO), Manama, Bahrain, 15–17 April 2019; pp. 1–5.
34. Mosaffa, A.H.; Farshi, L.G.; Infante Ferreira, C.A.; Rosen, M.A. Exergoeconomic and environmental analyses of CO2/NH3 cascade refrigeration systems equipped with different types of flash tank intercoolers. *Energy Convers. Manag.* **2016**, *117*, 442–453, doi:10.1016/j.enconman.2016.03.053.
35. Behzadi, A.; Arabkoohsar, A.; Yang, Y. Optimization and dynamic techno-economic analysis of a novel PVT-based smart building energy system. *Appl. Therm. Eng.* **2020**, *181*, doi:10.1016/j.applthermaleng.2020.115926.
36. Kumar Singh, K.; Kumar, R.; Gupta, A. Comparative energy, exergy and economic analysis of a cascade refrigeration system incorporated with flash tank (HTC) and a flash intercooler with indirect subcooler (LTC) using natural refrigerant couples. *Sustain. Energy Technol. Assess.* **2020**, *39*, doi:10.1016/j.seta.2020.100716.
37. Duffie, J.A.; Beckman, W.A. *Solar Engineering of Thermal Processes*, 4th ed.; John Wiley & Sons: Haboken, NJ, USA, 2013.
38. Shaker Al-Sayyab, A.K.; Al Tmari, Z.Y.; Taher, M.K. Theoretical and experimental investigation of photovoltaic cell performance, with optimum tilted angle: Basra city case study. *Case Stud. Therm. Eng.* **2019**, *14*, doi:10.1016/j.csite.2019.100421.
39. Bahaidarah, H.; Subhan, A.; Gandhidasan, P.; Rehman, S. Performance evaluation of a PV (photovoltaic) module by back surface water cooling for hot climatic conditions. *Energy* **2013**, *59*, 445–453, doi:10.1016/j.energy.2013.07.050.
40. Tiwari, A.; Sodha, M.S. Performance evaluation of solar PV/T system: An experimental validation. *Sol. Energy* **2006**, *80*, 751–759, doi:10.1016/j.solener.2005.07.006.
41. Lee, H.S. *Thermal Design: Heat Sinks, Thermoelectrics, Heat Pipes, Compact Heat Exchangers, and Solar Cells*; John Wiley & Sons: Haboken, NJ, USA, 2010; ISBN 0470496622.
42. Thulukkanam, K. *Heat Exchanger Design Handbook*; CRC Press Books: Boca Raton, FL, USA, 2013; ISBN 9781439842133.
43. Khosravi, A.; Koury, R.N.N.; Machado, L. Thermo-economic analysis and sizing of the components of an ejector expansion refrigeration system. *Int. J. Refrig.* **2018**, *86*, 463–479, doi:10.1016/j.ijrefrig.2017.11.007.
44. Tsatsaronis, G.; Moran, M.J. Exergy-aided cost minimisation. *Energy Convers. Manag.* **1997**, *38*, 1535–1542, doi:10.1016/S0196-8904(96)00215-4.
45. Liu, Z.; Liu, Z.; Yang, X.; Zhai, H.; Yang, X. Advanced exergy and exergoeconomic analysis of a novel liquid carbon dioxide energy storage system. *Energy Convers. Manag.* **2020**, *205*, 112391, doi:10.1016/j.enconman.2019.112391.
46. Tsatsaronis, G.; Morosuk, T.A. General exergy-based method for combining a cost analysis with an environmental impact analysis: Part I—theoretical development. In Proceedings of the ASME International Mechanical Engineering Congress and Exposition, Boston, MA, USA, 31 October–6 November 2008; pp. 453–462.
47. Li, F.; Chang, Z.; Li, X.; Tian, Q. Energy and exergy analyses of a solar-driven ejector-cascade heat pump cycle. *Energy* **2018**, *165*, 419–431, doi:10.1016/j.energy.2018.09.173.
48. Khalifa, A.H.N.; Faraj, J.J.; Shaker, A.K. Performance study on a window type air conditioner condenser using alternative refrigerant R407C. *Eng. J.* **2017**, *21*, doi:10.4186/ej.2017.21.1.235.
49. Al-sayyab, A.K.S. Experimental Evaluation of Window-Type Air-Conditioning Unit with New Expansion Device and R404A Alternative Refrigerant. *Int. J. Air-Cond. Refrig.* **2020**, *28*, 2050031, doi:10.1142/S2010132520500315.
50. Tello-Oquendo, F.M.; Navarro-Peris, E.; Gonzálvez-Maciá, J. Comparison of the performance of a vapor-injection scroll compressor and a two-stage scroll compressor working with high pressure ratios. *Appl. Therm. Eng.* **2019**, *160*, 114023, doi:10.1016/j.applthermaleng.2019.114023.